NASA-TM-86266 19840022261

NASA Technical Memorandum 86266

METHODS FOR ANALYSIS OF CRACKS IN THREE-DIMENSIONAL SOLIDS

I. S. RAJU AND J. C. NEWMAN, JR.

JULY 1984

National Aeronautics and
Space Administration

Langley Research Center
Hampton, Virginia 23665

METHODS FOR ANALYSIS OF CRACKS IN THREE-DIMENSIONAL SOLIDS

ABSTRACT

Various analytical and numerical methods used to evaluate the stress-intensity factors for cracks in three-dimensional (3-D) solids are reviewed. The review covers some of the classical exact solutions and many of the approximate methods used in 3-D analyses of cracks. The exact solutions for embedded elliptic cracks in infinite solids are discussed. The approximate methods reviewed are the finite element methods, the boundary-integral equation (BIE) method, the mixed methods (superposition of analytical and finite element method, stress-difference method, discretization-error method, alternating method, finite element-alternating method), and the line-spring model. The stress-intensity factor solutions for some commonly encountered 3-D crack configurations were compared. The solutions by various methods appear to show good agreement.

The finite-element method with singularity elements is the most widely used method. The BIE method only needs modeling of the surfaces of the solid and so is gaining popularity. The line-spring model appears to be the quickest way to obtain good estimates of the stress-intensity factors. The finite-element-alternating method appears to yield the most accurate solution at the minimum cost.

Comparisons between various methods have shown that accurate mode-I stress-intensity factors can be obtained. The choice of a particular method is only governed by the availability of computer programs and resources to obtain a solution.

INTRODUCTION

In aerospace, marine and nuclear structures, fatigue failures can occur from the initiation and propagation of cracks from holes, scratches or defects in the material. Such failures have caused loss of life, destruction of equipment, and severely reduced the life of these structures. To design against these failures, crack propagation lives and fracture strengths need to be accurately predicted. To make these predictions, stress-intensity factors are needed. Consequently, considerable research has been invested in the determination of stress-intensity factors. For generalized plane-stress and plane-strain conditions, many exact solutions have been developed. For complex two-dimensional (2-D) crack configurations, where exact solutions are not available, several approximate methods have been used to obtain the stress-intensity factors. These methods can be found in excellent reviews by Rooke et al. (ref. 1), Cartwright (ref. 2), and Hellen (ref. 3). Many stress-intensity factor solutions are now available in the form of compendia by Tada et al. (ref. 4), Rooke and Cartwright (ref. 5), and Sih (ref. 6).

A comprehensive review of aerospace structural failures completed by the United States Air Force in 1971 (ref. 7) showed that the origin of failures due to cracks, in order of frequency of occurrence to be (1) surface cracks, (2) corner cracks, and (3) cracks emanating from fastener holes. Such cracks propagate with elliptic or near elliptic shapes. These cracks are "truly" three-dimensional configurations. Two-dimensional approximations to these crack configurations are usually unsatisfactory and inaccurate. Accurate stress-intensity factors for these configurations, therefore, can be obtained only by solving 3-D boundary-value problems.

The purpose of this paper is to review various methods used for determining stress-intensity factors for cracked 3-D bodies. Because cracks tend to grow predominantly in mode-I, the symmetric opening mode, the review will be limited to determination of mode-I stress-intensity factors. First, some exact solutions for cracks in infinite solids are presented. Next, various approximate methods that have been used for the solution of the boundary-value problem of finite solids with cracks are reviewed. Third, the techniques used to extract the stress-intensity factors from these solutions are discussed. Last, various methods used to calculate the stress-intensity factors for through-the-thickness cracks, semi-elliptical surface cracks and quarter-elliptical corner cracks at holes are compared for the case of remote tensile loading.

LIST OF SYMBOLS

a	depth of crack
b	half-width of cracked plate (see Fig. 2)
c	length or half length of crack (see Fig. 2)
E	Young's modulus
F	boundary-correction factor
G	strain-energy release rate
h	half-height of cracked plate (see Fig. 2)
K_I, K_{II}, K_{III}	stress-intensity factor in Mode-I, Mode-II, and Mode-III, respectively
K_{ap}	apparent stress-intensity factor
N_∞, M_∞	remote membrane load and moment in the line-spring model
P	applied load
Q	shape factor for an elliptic crack
r, θ	polar coordinates with the origin at the crack tip

R	radius of the cylindrical pressure vessel
S	remote uniform tensile stress
t	thickness of the plate (see Fig. 2)
u, v	displacements along x- and y-directions, respectively
W	width of the compact specimens (see Fig. 11)
x, y, z	Cartesian coordinates
ν	Poisson's ratio
ϕ	parametric angle of the ellipse
$\{\sigma\}$	Cartesian stresses, $\{\sigma_x, \sigma_y, \sigma_z, \sigma_{xy}, \sigma_{yz}, \sigma_{zx}\}$

EXACT SOLUTIONS

In this section, the exact solutions for cracks in 3-D solids are summarized. The summary is limited to tensile loading and, hence, only mode-I stress-intensity factor solutions are discussed. Further, because surface and corner cracks propagate with elliptical or near elliptical shapes only elliptic cracks are considered here. For other crack shapes and loading see references 3-6, 8, and 9.

Circular (Penny-Shaped) Cracks

The problem of the stress distribution around a penny-shaped crack in an infinite solid was solved by Sneddon (ref. 10) using Fourier-Hankel transforms. He considered four types of loadings: (1) uniform normal pressure on the crack faces, (2) uniform pressure over a circular area, (3) concentrated ring loads, and (4) concentrated load acting at the center of the crack. All loads were symmetry about the crack plane. Smith, Kobayashi, and Emery (ref. 11) solved the problem of a penny-shaped crack subjected to any arbitrary pressure loading which can be expressed as a Fourier series.

Elliptical Cracks

Green and Sneddon (ref. 12) solved the stress distributions in an infinite body with an elliptical crack (see Fig. 1) using the known gravitational potential for a uniform elliptical disk. Irwin (ref. 13) then derived an exact expression for the mode-I stress-intensity factor around the elliptical crack subjected to uniform tension based on this exact solution. The stress-intensity factor along the boundary of the elliptical crack is

$$K_I = S\sqrt{\frac{\pi a}{Q}}\left[(a/c)^2 \cos^2 \phi + \sin^2 \phi\right]^{1/4} \tag{1}$$

where Q is the elastic shape factor for the ellipse and is related to the complete elliptic integral of second kind as

$$Q = \left[\int_0^{\pi/2} \left[(a/c)^2 \cos^2 \phi + \sin^2 \phi\right]^{1/2} d\phi\right]^2 \tag{2}$$

Kassir and Sih (ref. 14) derived the same results, equation (1), directly from the stress field.

When the semi-major and semi-minor axes, c and a, are equal, equation (1) reduces to the stress-intensity factor for a penny-shaped crack as

$$K_I = S\sqrt{\pi a}\,\frac{2}{\pi} \tag{3}$$

which is the exact solution by Sneddon (ref. 10).

The problem of an elliptical crack subjected to arbitrary pressure loading attracted much attention. Shah and Kobayashi (ref. 15) obtained the exact solution of an embedded elliptical crack subjected to a polynomial pressure load of the form

$$\sigma_y(x,0,z) = A_{00} + A_{10}x + A_{01}z + A_{20}x^2 + A_{11}xz + A_{02}z^2$$
$$+ A_{30}x^3 + A_{21}x^2z + A_{12}xz^2 + A_{03}z^3 \qquad (4)$$

The stress-intensity factor distribution along the crack front is given in terms of coefficients C_{ij} which are related to the coefficients A_{ij} in equation (4) by a matrix relation (see eq. 17 of ref. 15).

When all the coefficients A_{ij} except A_{00} are zero, and when all the coefficients A_{ij} except A_{10} are zero, Shah and Kobayashi's solution reduces to that of Green and Sneddon (ref. 12) and Kassir and Sih (ref. 14), respectively. For a penny-shaped crack subjected to sinusoidally varying pressure, the stress-intensity factors of Shah and Kobayashi reduce to those given by Smith et al. (ref. 11).

Since the pioneering work of Shah and Kobayashi in 1971, it was believed that the solution for embedded elliptical cracks subjected to arbitrary pressure loading is restricted to a cubic distribution like equation (4). However, in 1981, Vijayakumar and Atluri (ref. 16) derived a general solution procedure for an embedded elliptical crack, subjected to arbitrary crack-face tractions. In 1983, Nishioka and Atluri (ref. 17) presented a more detailed solution, as well as a general procedure for the evaluation of the required elliptical integrals found in the solution of reference 16. This analytical solution cannot be directly applied to embedded circular cracks because some individual terms in the solution take indeterminate form at $a/c = 1$. But the analytical solution for circular cracks ($a/c = 1$) can be derived from that of an embedded elliptical crack by taking appropriate limits for the integrals as the term $\sqrt{\frac{c^2 - a^2}{a^2}}$ tends to zero. Most analysts, however, prefer to

approximate circular cracks with $a/c = 0.98$ or 1.02 and use the general solution for an elliptical crack.

The exact solutions for elliptical cracks are limited to the completely embedded cracks in infinite solids.

APPROXIMATE METHODS

As pointed out earlier, failures usually originate as surface cracks, corner cracks, or cracks emanating from fastener holes. However, these configurations (see Fig. 2) are complex and, therefore, exact solutions for stress fields and stress-intensity factors are not available. To solve these 3-D boundary-value problems, a variety of techniques have been used. The techniques are (1) the finite-element method, (2) the boundary-integral equation method, (3) the mixed methods, and (4) the line-spring models. Some of these methods were aimed at solving for stress distribution in 3-D bodies. The methods for the extraction of stress-intensity factors were developed later. In the following sections, each of these methods is discussed. Although most of these methods can be used in mixed mode situations, the discussion is limited to mode-I problems.

Finite-Element Method

The finite-element method is a well-known method extensively used to solve 2-D and 3-D boundary-value problems. To solve crack problems, basically, two approaches are used - those based on conventional elements and those based on singularity elements.

Conventional Elements

In the conventional approaches, regular or standard finite elements are used to model the complete solid. The disadvantage of conventional elements

is that large numbers of elements are needed to accurately represent the stress field near the crack front (refs. 18-20).

Hall et al. (ref. 21) presented a 3-D macroelement technique. In this technique, the solid is first modeled into two or more substructures by 20-noded isoparametric elements and the region containing the crack by one simple 20-noded element. This region containing the crack is then modeled as a macroelement which contains a high density of nodes in the vicinity of the crack front and is compatible with the standard 20-noded elements adjoining it. With the macroelement, arbitrary 3-D configurations with cracks can be accommodated (refs. 21-23).

Singularity Elements

A square-root singularity exists along the crack front and, therefore, large stress gradients exist near the crack front. To delineate the stress field accurately in these regions, several special elements have been proposed. These elements have the required square-root singularity incorporated in their formulations. Some of the singularity elements proposed are described below.

Regular Displacement Models:

An element with the shape of an arbitrary pentahedron, with 6 nodes, was proposed by Tracey (refs. 24, 25) and was used in reference 26 (see Fig. 3(a) and 3(b)). With this element, the crack front is modeled with discrete linear segments. Usually about 8 singularity elements around the crack front are used in symmetric crack problems (ref. 26). The remainder of the solid is modeled with 8-noded isoparametric hexahedrons (refs. 24-32). The singular pentahedron element is of the nonconforming type.

Stern and Becker (ref. 33) and Blackburn and Hellen (ref. 34) proposed a 6-noded and 15-noded singular element (see Figs. 3(c) and 3(d)). The 15-noded

element is a pentahedron with curved sides with 6 corner nodes and 9 midside nodes. Because of the curved sides the crack front can be approximated with parabolic arcs. References 33 and 34 used 6 and 4 singularity elements, respectively, around the crack front for symmetric crack problems. This singularity element is compatible with the standard 20 noded isoparametric elements that are used to model the remainder of the solid.

Enriched Displacement Models:

Benzley (ref. 35) proposed the concept of enriched singularity elements for 2-D crack problems. The enrichment process can be explained as follows. Consider an isoparametric quadrilateral at a crack tip. The displacement functions assumed for this element are like

$$u(x,y) = \sum_{j=1}^{4} N_j u_j \quad \text{and} \quad v(x,y) = \sum_{j=1}^{4} N_j v_j \tag{5}$$

where u and v are the displacements at any point inside the element. The u_j and v_j are the displacements at node j. N_j is the shape function. Benzley proposed to "enrich" the element by adding the near field displacements from the exact solution at the crack tip as

$$u(x,y) = \sum_{j=1}^{4} N_j u_j + K_I\left(Q_{Iu} - \sum_{\alpha=1}^{4} N_\alpha \bar{Q}_{Iu_\alpha}\right) + K_{II}\left(Q_{IIu} - \sum_{\alpha=1}^{4} N_\alpha \bar{Q}_{IIu_\alpha}\right) \tag{6}$$

and similar equation for the v-displacements. In equation (6), K_I and K_{II} are the unknown stress-intensity factors, $\bar{Q}_\alpha$ are the values of Q evaluated at the node α.

The Q functions in equation (6) are chosen to be the near field displacements at a crack tip as,

$$
\begin{aligned}
Q_{Iu} &= \frac{2(1+\nu)}{E}\sqrt{\frac{r}{2\pi}}\cos\frac{\theta}{2}\left[\frac{\kappa-1}{2}+\sin^2\frac{\theta}{2}\right] \\
Q_{Iv} &= \frac{2(1+\nu)}{E}\sqrt{\frac{r}{2\pi}}\sin\frac{\theta}{2}\left[\frac{\kappa+1}{2}-\cos^2\frac{\theta}{2}\right] \\
Q_{IIu} &= \frac{2(1+\nu)}{E}\sqrt{\frac{r}{2\pi}}\sin\frac{\theta}{2}\left[\frac{\kappa+1}{2}+\cos^2\frac{\theta}{2}\right] \\
Q_{IIv} &= \frac{2(1+\nu)}{E}\sqrt{\frac{r}{2\pi}}\cos\frac{\theta}{2}\left[-\frac{\kappa-1}{2}+\sin^2\frac{\theta}{2}\right]
\end{aligned}
\tag{7}
$$

where $\kappa = 3 - 4\nu$ for plane strain and $(3 - \nu)/(1 + \nu)$ for plane stress. The r and θ are the polar coordinates with their origin at the crack tip. Equations 7 represent the displacement components along x- and y-directions in mode-I and mode-II (refs. 4, 6).

The displacement interpolation functions as described by equation 6 do not maintain interelement compatibility. Benzley suggests multiplication of the last two terms in equation (6) by functions which are zero on the element boundaries which adjoin the regular elements. Thus, Benzley's enriched element would be a compatible element and, therefore, assures monotonic convergence. The stress-intensity factors K_I and K_{II} are unknowns in addition to the nodal displacements. Thus, the enriched elements have the advantage that no other methods of extraction of stress-intensity factors are necessary after the finite-element solution is obtained. This concept of the enriched elements was used by Gifford and Hilton to develop a 12-noded quadilateral element for 2-D crack problems (ref. 36), and by Hilton et al. to develop a 15-noded pentahedron element with curved faces (refs. 37-39) for 3-D crack

problems. The stress-intensity factors K_I, K_{II}, and K_{III} are unknowns in addition to the nodal displacements and will be available when the finite-element solution is obtained.

Quarter-Point Elements:

Henshell and Shaw (ref. 40) and Barsoum (refs. 41, 42) proposed that by displacing the midside nodes from their normal position in an 8-noded quadrilateral isoparametric element, one can simulate a square-root singularity at a corner node. They showed that the necessary position of the displaced node should be at a distance of one-quarter of the length of the side from the corner node where the square-root singularity is needed. Henshell and Shaw (ref. 40) suggested using an 8-noded element and 20-noded quarter-point elements as in Figures 3(e) and 3(f) for 2-D and 3-D problems, respectively. Barsoum (refs. 41, 42) suggested collapsing one side of an isoparametric element to form a triangular element with quarter-point nodes as in Figure 3(g) and collapsing one face of a 20-noded isoparametric element to form a 15-noded pentahedron element with quarter-point nodes as in Figure 3(h) for 3-D problems. These quarter-point elements are attractive because of the ease with which they can be implemented in a general purpose program. These elements are extensively used by Ingraffea and his coworkers (refs. 43-46), Hechmer and Bloom (ref. 47), and Wu (ref. 48).

Hybrid Elements:

In addition to the elements described above, two types of hybrid singularity elements were also developed. They are the stress-hybrid and displacement-hybrid elements. The advantage of these singularity elements is that the stress-intensity factors K_I, K_{II}, and K_{III} are obtained as a part of the solution.

Pian and Moriya (refs. 49, 50) proposed assumed stress-hybrid elements. In these elements, the stress singularities are represented by the stress-intensity factors K_I, K_{II}, and K_{III} and the near field 2-D stress solutions at the crack front. Other assumed stress terms are simple polynomials which satisfy equilibrium and the stress-free conditions on the crack faces. In addition, displacements along the element boundaries are assumed such that they are compatible with the standard elements. The complementary energy is minimized to obtain the element stiffness. Following the procedures laid out by Pian and Moriya, Kuna (ref. 51) developed a 20-noded hexahedron (assumed stress singularity) element. The crack front is approximated by linear segments and each segment is surrounded by a group of four singularity elements for the general case and two for the symmetric case (refs. 49-51).

The displacement formulation for hybrid elements is similar to that of the stress formulation. In the displacement formulation, however, one assumes a compatible displacement field within the element as well as another set of independent displacements and tractions on the boundaries of the element. The singular stress field in the element is incorporated by the stress-intensity factors (K_I, K_{II}, and K_{III}) and the near field displacements at a smooth crack front as given in reference 14. (Note that the near field solution for the displacements for the 3-D case can be obtained by superposition of all three modes under plane-strain conditions with $\kappa = 3 - 4\nu$). On the element boundaries, displacements are assumed which are compatible with standard adjoining elements. A modified variational principle (ref. 52) is used to obtain the element stiffness matrices of these singularity elements. Tong and Atluri (ref. 52) and Atluri and Kathiresan (refs. 53-59) developed and extensively used these displacement-hybrid singularity 20-noded hexahedron elements. The crack front can be approximated by parabolic arcs and each arc is

surrounded by a group of four singularity elements for the general case and two for the symmetric case (ref. 59).

Boundary-Integral Equation (BIE) Method

Any linear elasticity problem can be solved using two second-order tensor kernels defined on the boundary (refs. 60-64). These kernels depend only on the configuration being analyzed. These two kernels allow the calculation of displacements and tractions at the boundary by an integral equation. The interior displacements and stresses can then be calculated in terms of the two kernels, the boundary displacements, and boundary stresses.

The BIE method uses the reciprocal theorem of elasticity together with the solution of a point load in a infinite solid. The reciprocal theorem relates the known point load solution to the solution of the desired problem. In the numerical solutions by the BIE method, the boundary of the solid is modeled with elements similar to the 2-D finite elements. Therefore, 3-D modeling of a solid is reduced to 2-D modeling of boundary surfaces. However, in contrast to the finite-element analysis, the matrix involving the linear algebraic simultaneous equations obtained in the BIE method is not symmetrical and is fully populated. Also, the BIE method is inferior to finite-element method when stresses at many points inside the solid are desired (ref. 62). But, the BIE method is gaining popularity for 3-D problems. Two-dimensional elements like the 2-D finite elements including quarter-point elements can be used along the crack front.

The BIE method has been widely used by Cruse (refs. 62, 65), Heliot et al. (refs. 66, 67), Cruse and Wilson (ref. 68), Harris and Lin (ref. 69), Cruse and Vanburen (ref. 70), and Lange (ref. 71), for problems of through cracks and surface cracks in plates and cylindrical vessels.

Mixed Methods

As pointed out earlier, finite-element analyses of 3-D crack problems involve large number of degrees of freedom because of refined meshes along the crack fronts. Further, modeling and data input become difficult and the number of equations can exceed the capacity of average computer systems. Therefore, several techniques of reducing degrees of freedom have been proposed. These techniques use either several finite-element solutions or combine two different methods, one of which is usually a finite-element solution. The mixed methods that have been proposed are

1. Superposition of analytical and finite element methods
2. Stress-difference method
3. Discretization error method
4. Alternating method
5. Finite element - alternating method

An excellent summary and comparisons of the first three methods can be found in reference 20. For completeness all these three methods are presented in the appendix. In this section the widely used alternating method and the finite element-alternating method are discussed.

Alternating Method

The alternating method (refs. 72-74) uses two basic analytical elasticity solutions for infinite and semi-infinite solids. The first solution, Solution 1, is that for an elliptical crack in a infinite solid; the crack faces are subjected to variable normal loads (refs. 15, 72). The second solution, Solution 2, is that of an uncracked semi-infinite body subjected to uniform normal and shear stresses over a rectangular portion of the free surface (ref. 75).

The analytical solution to the problem of an elliptical crack in an infinite solid, Solution 1, with normal loading on the crack faces was obtained by Shah and Kobayashi (refs. 72, 73). In this work, however, the variation of the loading normal to the crack faces is limited to a cubic function in the x- and z-coordinates (see Fig. 1) as

$$\sigma_y(x,0,z) = A_{00} + A_{01}x + A_{02}x^2 + A_{20}z^2 + A_{21}xz + A_{03}x^3 \qquad (8)$$

The stresses and the stress-intensity factor may be computed directly from a lengthy set of equations involving elliptical and Jacobian elliptical integrals if the constants A_{ij} in equation (8) are known.

The alternating method is an iterative method in which stresses on the external surfaces of the solid and the crack faces are reduced to zero by alternating between Solution 1 and Solution 2. The logic for the iterative steps is explained in the flow chart in Figure 4. In this method, the external surfaces of the solid are modeled by rectangular regions. The stresses in each of these rectangular regions due to Solutions 1 and 2 are evaluated for each iteration and are used as shown in Figure 4.

Shah and Kobayashi (refs. 72, 73) modeled the front and back faces with rectangular domains as shown in Figure 5. Very similar rectangular domain idealization was used by Smith (ref. 74). Detailed discussion on the approaches in references 72-74 can be found in the evaluation by McGowan (ref. 22).

This method needs only coarse idealizations of the front and back faces and, hence, the number of degrees of freedom in the problem are small. Further, the stress-intensity factors are directly obtained as a part of the solution.

Finite-Element-Alternating Method

As noted earlier, the alternating method uses the analytical solution (refs. 11, 15, 72) for an embedded elliptical crack in an infinite solid. This analytical solution has been limited to cubic variation of normal pressure on the crack surfaces. Recently, a general solution procedure has been derived (ref. 16) for the problem of an infinite elastic medium with an embedded elliptical crack in which the the faces of the crack are subjected to arbitrary variations of normal and shear tractions. Nishioka and Atluri (ref. 17) presented a more detailed solution and a general procedure for the evaluation of the required elliptic integrals found in the solution of reference 16.

Utilizing this analytical solution, Nishioka and Atluri (refs. 76, 77) proposed a finite-element-alternating method. The procedure is summarized in Figure 6. A very similar procedure was used by Browning and Smith (ref. 78) and Smith and Kulgren (ref. 79) except that they used the analytical solution of references 15 and 72.

This method needs only coarse finite element models because the singularity at the crack front is modeled by the analytical solution. Further, the stress-intensity factors are directly obtained as a part of the solution.

Line-Spring Model

The line-spring model (LSM) was originally proposed by Rice and Levy (ref. 80) for the analysis of surface crack problems. The 3-D crack problem is reduced to a 2-D plate (or shell) theory problem. Consider the surface-crack configuration like Figure 2(a). Figure 7(a) shows the cracked plane of this plate. The surface-cracked configuration is idealized as a through-the-thickness center crack of length 2c in a plate with a series of line springs across the crack faces (see Fig. 7(b)). The remote loads N_∞ and M_∞ on the

surface-cracked plate are applied to the plate in Figure 7(b). The surface crack in Figure 7(a) has an uncracked ligament of $t - a(x)$ at any distance x from the center ($a(x)$ describes the depth of the surface crack at any distance x from the center). The 2-D idealization must account for the transmission of membrane loads N_∞ and M_∞ across the crack faces. That is, the stiffness of the line springs should vary with the coordinate x. To determine the stiffness of these springs the following procedure was followed.

Due to the external loads, the middle surface of the plate on one side of the line spring displaces by an amount δ and rotates an angle α, relative to the other side. The values of δ and α at any point are considered to be functions of the membrane loads and bending moment per unit length which are transmitted across the spring at that location, x. Then, the stiffness of the spring at x is the inverse of the compliance matrix which relates $\{\delta\}$ and $\{N\}$ as

$$\begin{bmatrix} \delta(\xi) \\ \alpha(\xi) \end{bmatrix} = \left[C(\xi)\right] \begin{bmatrix} N(\xi) \\ M(\xi) \end{bmatrix} \tag{9}$$

where $\xi = x/c$. Rice and Levy (ref. 80) proposed that the compliance of these springs (Eq. 9) can be obtained from a plane-strain solution of a single-edge cracked plate (Fig. 7(c)) of width t and crack length a subjected to an axial force N and bending moment M per unit thickness. Note that the compliance is a function of the crack depth.

At each x-location, the crack-depth $a(x)$ is first established. Then, for this crack depth the compliance matrix [C] of equation (9) is calculated from the single-edge crack solution with an edge-crack $a(x)$ in a plate of thickness t. Inverse of the compliance matrix [C] will yield the desired

stiffness matrix of the line-spring at that x-location. This procedure is used to determine the stiffnesses of the line-springs from $x = -c$ to $x = c$.

These line-spring elements are then used across the faces of the center-crack (see Fig. 7(b)). The center-cracked plate with the line-springs across its crack faces is then subjected to the remote loads N_∞ and M_∞. The solution of this boundary value problem yields the relative displacements $\delta(x)$ and $\alpha(x)$. From these displacements the loads $N(x)$ and $M(x)$ at any station x can be calculated by equation (9). The stress-intensity factor $K_I(x)$ is then calculated from

$$K_I(x) = \sqrt{\pi a(x)}\left[F_1\left(\frac{a(x)}{t}\right)\frac{N(x)}{t} + F_2\left(\frac{a(x)}{t}\right)\frac{6M(x)}{t^2}\right] \tag{10}$$

The functions F_1 and F_2 are obtained from the plane-strain solutions for a single-edge cracked plate in tension and bending, respectively (refs. 4-6).

The boundary value problem of Figure 7(b) was solved using the finite-element method by German et al. (ref. 81) and using integral equations in references 80 and 82-85. With this model, German et al. (ref. 81), Parks et al. (ref. 82), Delale and Erdogan (refs. 83, 84), and Rice (ref. 85) analyzed the surface crack in plates and cylindrical vessels.

A model very similar to the line-spring model called the slice-synthesis model was developed by Dill and Saff (ref. 86). They also applied this model to surface cracks in plates.

EXTRACTION OF STRESS-INTENSITY FACTORS

After the boundary-value problem is solved, one has to extract the stress-intensity factors from the solution. In some formulations using the finite-element method, the stress-intensity factors are included in the elements as the unknown parameters. In such cases, the stress-intensity factors

are available when the boundary-value problem is solved. The enriched elements (refs. 35-39), the stress-hybrid elements (refs. 49-51), and the displacement-hybrid elements (refs. 52-55) give stress-intensity factors directly from the solution.

When other elements are used, however, the stress-intensity factors must be extracted from the finite-element solution. Three methods are widely used. They are the crack-opening displacement (COD) method, the force method, and the virtual-crack extension method. These methods are briefly discussed below.

Crack-Opening Displacement Method

In this method, the COD just behind the crack front is compared to the corresponding 2-D case to evaluate the stress-intensity factor. If r is the radial distance measured normal from the crack front at station i (see Fig. 8), then the 2-D solution assuming plane strain gives

$$v = \frac{4(1 - \nu)^2}{E} K_I \sqrt{\frac{r}{2\pi}} \tag{11}$$

where v is the one-half of the COD at a distance r from the crack front.

In the COD method, two approaches are used. In the first approach, Approach 1, the crack-opening displacement at the node next to the crack front is used in equation (11) to calculate K_I. In the second approach, Approach 2, the COD values at various distances from the crack front are used to calculate apparent stress-intensity factors, K_{ap}. Linear regression is used on the K_{ap} against r plot (Fig. 8(b)) to compute the value of K_I at the intercept, $r=0$.

The first approach, utilizing one node, is extensively used with quarter-point elements (refs. 42-48), the conventional finite-element method

(refs. 18-20) and singularity elements (ref. 87). The second approach is used with singularity elements (refs. 34, 40, 88).

The main disadvantage of this method is that one has to assume a state of stress, either plane stress or plane strain. The stress-intensity factors calculated from the assumption of plane stress and plane strain differ by a factor $(1 - \nu^2)$, the plane-strain assumption yielding the higher value. The factor $(1- \nu^2)$ translates to a 9 percent difference for a Poisson's ratio of 0.3. Most analysts prefer to use the plane-strain assumption all along the crack front and the plane-stress assumption in the region where the crack meets the free surfaces.

Force Method

In this method, the forces ahead of the crack front and normal to the crack plane are used to evaluate stress-intensity factors.

In contrast to the near-field displacements at the crack tip (in the 2-D case), the near field stresses ahead of the crack tip are identical for plane stress and plane strain. Therefore, use of the 2-D stress solution ahead of the crack tip would eliminate the assumption of either plane stress or plane strain. However, the accuracy of stresses in a finite element solution is not as good as that for displacements. But the accuracy of nodal forces computed in a finite-element solution is the same as that of displacements. Therefore, Raju and Newman (refs. 26 and 27) used the finite-element forces ahead of the crack front and normal to the crack plane, and compared these forces to those obtained by integrating the near-field stresses from the 2-D solution. The stress-intensity factor is evaluated, as in the COD method, by plotting the K_{ap} against radial distance r from the crack front and extrapolating to $r=0$ as in Figure 8(b). The method thus avoids the assumption of plane stress or plane strain. This method was extensively used in references 26-32.

Virtual Crack Extension Method

In this method, the strain-energy release rate (G) for the cracked configuration is calculated and then the K values are evaluated from G. The strain-energy release rate is obtained by taking the difference in the strain energy of the structure divided by incremental crack length Δc, $G = -\frac{\Delta u}{\Delta c}$. In the conventional finite-element analysis, this requires two runs with crack lengths c and $c + \Delta c$.

Parks (ref. 89) and Hellen (ref. 90) proposed similar algorithms which require only one run at crack length c. The 2-D problem is first solved by a finite-element method. Then the crack length c is incremented by amount Δc. When the crack length is $c + \Delta c$, nodes within, but not on the contour Γ_1 (see Fig. 9), get shifted by an amount Δc. However, all nodes within and on the contour Γ_0 simply get shifted by Δc and therefore suffer no change in energy. The only change in the energy is due to changes in the element configuration between contours Γ_0 and Γ_1. Therefore, the strain-energy release rate is

$$G = \frac{1}{2} \{u\}^T \left[\frac{1}{\Delta c} \left\{ [k]_{c+\Delta c} - [k]_c \right\} \right] \{u\} \tag{12}$$

where $\{u\}$ are the displacements obtained from the original loading and with a crack length of c. The $[k]_{c+\Delta c}$ and $[k]_c$ are the assembled stiffness matrices of elements between the contours Γ_0 and Γ_1. They are calculated with coordinates corresponding to crack lengths $c + \Delta c$ and c. The stress-intensity factor K_I can be calculated from G by the relations

$$G = \frac{K_I^2}{E} \quad \text{for plane stress}$$

$$= \frac{K_I^2}{E}(1 - \nu^2) \quad \text{for plane strain} \tag{13}$$

In this method, the crack extensions Δc can be very small, of the order of 10^{-3} to 10^{-5} times the crack length c. For 3-D analysis, the extension is straightforward and is discussed in detail in references 89 and 90. Again, to obtain the stress-intensity factor by this method, an assumption of either plane stress or plane strain needs to be made because of equation 12.

The virtual crack extension method was extensively used by Hall et al. (ref. 21), McGowan and Raymund (ref. 23), Hellen (ref. 90), and Blackburn and Hellen (ref. 34).

COMPARISONS

The methods outlined earlier were used to obtain stress-intensity factors for various cracked solids. Broad comparisons between different methods are not possible because the investigators did not work identical configurations and loading. However, the following specific configurations subjected to tensile loading have been studied by numerous investigators.

1. Compact specimen
2. Semi-elliptical surface crack in a plate
3. Semi-elliptical surface crack in cylindrical pressure vessels
4. Quarter-elliptical corner cracks from holes

The solutions for each of these configurations will be compared in this section.

Compact Specimens

Compact specimens shown in Figure 10 represent the simplest 3-D configurations with cracks. These specimens have through-the-thickness cracks with straight crack fronts. Several investigators have analyzed these configurations with varying degree of success. All investigators showed that the stress-intensity factor, K_I, at the midplane of the specimen is higher than that at the surface. However, the K_I value at the midplane computed by various investigators disagreed by as much as 9 percent. In reference 87, Tseng reviewed these results. Table 1, taken from reference 87, summarizes the results. A recent result for configuration of Type C (see Fig. 10) is added to the table. This table presents the nondimensional stress-intensity factor, F, obtained by various investigators normalized by the F value obtained from plane-strain collocation methods. Based on the results in Table 1, Tseng concluded that (1) COD method using Approach 1 yields accurate results, (2) superposition and 15-noded singular elements are reliable, and (3) pronounced error may result unless care is taken in selecting the type of singularity element.

Tseng's conclusion 3 was based on the lower values of F at the midplane calculated by Tracey (ref. 25), Raju and Newman (ref. 26), and Kathiresan (ref. 59). The reason for these lower values, however, is not because of the singularity elements used but because of the inadequacy of the finite-element model to represent the bending that occurs in the compact specimen. In reference 91, Raju and Newman analyzed the compact specimen Type C (see Fig. 10). (Note that the Type C configuration has a different height H compared to Type A and Type B configurations.) They refined the mesh on a z = constant plane in a 2-D analysis until they were within 2 percent of the plane-strain value. Then they performed a convergence study in the thickness direction in

a 3-D analysis to model one-quarter of the specimen. Table 2 presents the results of the convergence study. The F value at the midplane from the 2-layer model differed from that with the 8-layer model by only 1 percent. Therefore, the modeling on a z = constant plane is more important in this problem than the modeling in the thickness direction.

Table 3 presents the effect of thickness of the specimen. Surprisingly, the specimens with W/B = 5 and W/B = 1 gave nearly same F values at the midplane and these values are slightly lower than that for W/B = 2. Therefore, there appears to be a slight thickness dependence on the F value at the midplane.

The two configurations, Type A and Type B, analyzed by the investigators in Table 1 corresponds to the one with W/B = 2. For this configuration, Tseng (ref. 87) showed that the maximum F value for the finite-thickness compact specimen should be about 8 percent higher than the plane strain value. Similar conclusion was reached by Raju and Newman (ref. 91) using Type C configuration with W/B = 1. Therefore, it appears that most of the available singularity elements and K-evaluation procedures can yield accurate results provided the finite-element models can adequately represent the bending that occurs in the compact specimen. Furthermore, for the same accuracy some singularity element models need fewer degrees of freedom compared to other singularity element models.

Semi-Elliptical Surface Crack in a Plate

The second three-dimensional cracked configuration studied by several investigators is that of a semi-elliptical surface crack in a finite plate (Fig. 2(a)). Several investigators worked the problem of a semicircular (a/c = 1) surface crack, with shallow crack depths, that is, a/t < 0.2. Pian and Moriya (ref. 50) used stress-hybrid singularity elements. Tracey

(refs. 24, 25) used the 6-noded singularity element with COD method using Approach 1. Blackburn and Hellen (ref. 34) used a 15-noded singularity element and the virtual crack extension method. Yagawa and Nishioka (ref. 92) used the superposition method. These solutions are in excellent agreement with one another. Ando and Yagawa (ref. 20) reviewed and compared various solutions by mixed methods for this problem. The results by various methods show qualitative agreement but the stress-intensity factors differed in some cases by more than 10 percent.

In 1979, Newman (ref. 93) reviewed the solutions for the surface crack problem obtained by analytical methods, experimental methods, and by engineering estimates. He limited the review to the solutions which were applicable to wide ranges of crack shapes ($0.2 \leq a/c \leq 1$) and sizes ($0 \leq a/t \leq 0.8$). The analytical methods reviewed were: alternating method (refs. 72-75, 78, 94), line-spring model (ref. 80), and the finite element method (refs. 27, 29). For shallow cracks, $a/t \leq 0.3$, and near semi-circular cracks, $0.6 \leq a/c \leq 1$, the stress intensity factor at the maximum depth point ($\phi = \pi/2$) by various methods showed good agreement (5 percent) with one another. However, for deeper cracks, $a/t > 0.3$, and for semi-elliptical cracks, $0.2 \leq a/c \leq 0.6$, the stress-intensity factors by various methods showed considerable disagreement (20 to 80 percent). Newman (ref. 93) attributed some of the discrepancies between the results to the improper prescription of boundary conditions.

In 1976, at a workshop at Battelle's Columbus Laboratory three "Benchmark Problems for Three-Dimensional Fracture Analysis" were proposed (ref. 95) for use as standards for comparing analysis methods. One of the benchmark problems, Benchmark Problem 1, was the problem of a semi-elliptical surface crack in a finite plate. Only a few analysts have worked the wide range of parameters suggested by Hulbert (ref. 95). Atluri and Kathiresan (refs. 53, 54)

used a displacement-hybrid singularity element. Raju and Newman (refs. 27, 29) used the 6-noded singularity element and a force method to evaluate the stress-intensity factors. McGowan and Raymund (ref. 22) used the macro-element approach (ref. 21) in conjunction with the virtual crack extension method for extracting stress-intensity factors. Heliot et al. (ref. 96) used the boundary-integral method with the COD method (Approach 1). Shah and Kobayashi (refs. 72, 73) and Smith and Sorensen (ref. 94) used the alternating method. These six solutions were critically evaluated and reviewed by McGowan in reference 22. McGowan's comparison of various solutions for crack shape of $a/c = 0.5$ and a crack depth of 0.75 is shown in Figure 11. For this deep crack and a shallow crack ($a/t = 0.25$) there is good agreement among the six different solutions. In particular, the finite-element solutions of references 27, 29, 53, and 54 and the boundary-integral equation method (ref. 96) solutions were in very good agreement (5 percent) with one another. Based on these comparisons, McGowan suggested a best estimate curve and a band of 3 percent for the stress-intensity factor distributions along the crack front (see Fig. 11).

Since the review by McGowan, as pointed out earlier, Nishioka and Atluri (ref. 17) used the finite-element-alternating method and analyzed the benchmark problem. Their results showed excellent agreement with the benchmark estimate of McGowan. Very recently, Wu (ref. 48) analyzed the benchmark problem with quarter-point elements using the COD method (Approaches 1 and 2). He compared his results for $a/c = 0.5$ and $a/t = 0.25$ and 0.75 with the benchmark estimate of McGowan. Excellent agreement is reported in reference 48. Wu also compared his results with the interpolated values from reference 29. For the majority of cases, the agreement is excellent (1 to

3 percent). For the special case of $a/c = 0.2$ and $a/t = 0.8$, Wu's results were 10 to 15 percent lower than those of reference 29.

The surface crack problem with a slightly different configuration than the benchmark problem was also analyzed with the line-spring models. German et al. (ref. 81), and Parks et al. (ref. 82) analyzed surface cracks with $a/c = 0.2$ and 0.667 with a/t ratios from 0.2 to 0.8. Delale and Erdogan (ref. 83) and Dill and Saff (ref. 86) analyzed surface cracks with $a/c = 0.2$ and $a/t = 0.4$ to 0.8. The results of references 81 and 82 at the deepest point are in very good agreement (4 percent) with those of reference 27. The differences between the results of (ref. 81 or 82) and (ref. 27) increase near the free surface ($\phi = 0$). Also, the results for the shallow cracks are in better agreement than those for the deep cracks. Furthermore, for $a/c = 0.667$, the agreement is not as good as those for $a/c = 0.2$. The largest disagreement was observed when $a/c = 0.667$ and $a/t = 0.2$. This is not surprising since this configuration taxes the assumptions made in the line-spring model. Delale and Erdogan (ref. 84) and Dill and Saff (ref. 86) compared their results with those of Raju and Newman (ref. 27). Again very good agreement (3 percent) is observed for all three a/t ratios. Table 4 summarizes the normalized stress intensity factors at the deepest point ($\phi = \pi/2$) of a semi-elliptical crack with $a/c = 0.2$ obtained by the three line-spring models and compares with those of references 27 and 29.

Semi-Elliptical Surface Cracks in Cylindrical Pressure Vessels

The third 3-D crack configuration studied by several investigators is that of a semi-elliptical surface crack in a cylindrical pressure vessel (see Fig. 12). The configuration extensively studied is a cylinder of $R/t = 10$ with an internal surface crack with $a/c = 1/3$. This is a standard configuration recommended by the ASME Boiler and Pressure Vessel Code.

In contrast to the Benchmark Problem 1, several investigators chose to load the crack faces. They applied four crack face distributions, uniform, linear, quadratic and cubic, to the crack faces as

$$\sigma_j = (z/a)^j \quad \text{for} \quad j = 0,\ 1,\ 2,\ 3 \tag{14}$$

where z is measured from the crack mouth toward the crack front (see Fig. 13(c)). The stress-intensity factors are expressed as

$$K_I = \sqrt{\frac{\pi a}{Q}}\, G_j \quad \text{for} \quad j = 0,\ 1,\ 2,\ 3 \tag{15}$$

The influence coefficient G_j corresponds to the jth stress distribution.

Several investigators obtained the influence coefficients G_j for each of the jth crack face loadings. McGowan and Raymund (ref. 23) used the macroelement approach with the virtual crack extension technique for evaluating the stress-intensity factors. Atluri and Kathiresan (refs. 56, 57) used the displacement-hybrid singularity element. Raju and Newman (refs. 31, 32) used the 6-noded singularity element and the force method to evaluate the stress-intensity factors. Heliot et al. (ref. 67) used the boundary-integral equation method and the COD method (Approach 1). Nishioka and Atluri (ref. 77) used the finite element-alternating method. A typical finite element model for this problem (ref. 31) is shown in figure 13.

Figure 14 compares the influence coefficient distributions obtained in references 23, 31, 32, and 67 for a deep crack, $a/t = 0.8$, for various crack face loading distributions. The influence coefficient distributions of reference 67 agreed very well with those of references 31 and 32. The maximum discrepancy is about 2 percent. The finite element results of reference 23 are within 8 percent of the results of Heliot et al. (ref. 67). Similar

agreement between these three investigators were also noted for $a/t = 0.5$ in reference 32. The finite-element-alternating method was also applied to this configuration in reference 76. The influence coefficients obtained with this method agreed well with those reported in references 32 and 67 for both $a/t = 0.5$ and 0.8. Atluri and Kathiresan (ref. 56) using the displacement-hybrid singularity element analyzed the same configuration but with internal pressure loading. Their stress-intensity factors were about 7, 8, and nearly 0 percent, lower than those in reference 67 for $a/t = 0.25$, 0.5 and 0.8, respectively.

The line-spring model was also used to analyze the cylindrical vessel configuration. German et al. (ref. 81) analyzed a cylindrical vessel ($R/t = 10$) subjected to internal pressure. They compared their solution for $a/c = 1/3$ and $a/t = 0.2$ and 0.8 with that of Newman and Raju (ref. 31). At the maximum depth point ($\phi = \pi/2$), the results agreed within 3 percent for $a/t = 0.2$ and within 1 percent for $a/t = 0.8$. Delale and Erdogan (ref. 83) analyzed the same cylindrical vessel subjected to internal pressure with a longitudinal surface crack with $a/c = 0.2$ and $a/t = 0.2$ and 0.8. At the deepest point of the crack ($\phi = \pi/2$), their solution is about 5 and 9 percent higher than that of reference 31 for $a/t = 0.2$ and 0.8, respectively.

The complex configuration of a semi elliptical surface crack in a cylinder appears to be well analyzed by various methods. The agreement between several investigators is good.

Quarter-Elliptical Corner Cracks from Holes

A configuration that is more complex than the previous three, is that of a quarter-elliptical corner crack emanating from a hole. Figure 2(c) shows the configuration studied by several investigators. Shah (ref. 97) used the alternating method and enginering estimates, Smith and Kulgren (ref. 79) used

finite-element-alternating method, Kathiresan (ref. 59) used the displacement hybrid-singularity element, Hechmer and Bloom (ref. 47) used quarter-point elements with the COD method (Approach 2). Raju and Newman (ref. 28) analyzed the configuration with 6-noded singularity elements and obtained the stress-intensity factors by the force method. Recently, Nishioka and Atluri (ref. 76) applied the finite-element-alternating method to the corner crack configuration.

For a quarter-circular corner crack ($a/c = 1$, $a/t = 0.5$, and $R/t = 0.5$) figure 15 compares the stress-intensity factors obtained by several investigators. Smith and Kulgren's (ref. 79) results in this figure were obtained from interpolation between their results of $a/c = 0.75$, 1.5 and 2.0. Their results and the results of Raju and Newman (ref. 28) are in very good agreement (less than 5 percent). The results of Shah (ref. 97) and Kathiresan (ref. 59) are about 10 percent and 15 percent lower than those of reference 28, respectively.

Hechmer and Bloom (ref. 47) analyzed a shallower crack ($a/t = 0.2$) than that discussed in Figure 15 and their results are about 10 to 20 percent higher than the corresponding results of reference 28 (see Fig. 8(a) of ref. 28).

The corner cracks in Figure 2(c) tend to grow faster along the hole boundary rather than on the front face under cyclic loading. Therefore, the stress-intensity factors for cracks with $a/c > 1$ are important. Raju and Newman (ref. 28) and Nishioka and Atluri (ref. 76) analyzed one such case. They analyzed the configuration of quarter elliptical corner cracks with $a/c = 2$, $R/t = 0.5$ for three crack depths, and $a/t = 0.2$, 0.5 and 0.8 under pin loading. The pin loading was assumed to be applied by normal stresses on the hole boundary, σ_n (see Fig. 16) as

$$\sigma_n = \frac{3P}{4Rt} \sin^2 \theta \tag{16}$$

where P is the total applied force acting in the y-direction over the arc from $\theta = 0$ to π. The comparison of the stress-intensity factors by these two methods is shown in Figure 17. (The results of Raju and Newman in Figure 17 for $a/t = 0.2$ and 0.5 are corrected results. The originial results of reference 28 for these crack depths with $a/c = 2$ were in error due to a computer input error.) Fair agreement is observed between the two sets of results except near the region, where the crack intersects the edge of the hole ($\phi = \pi/2$). The drop-off of the stress-intensity factors of reference 28 was attributed to the boundary-layer effect and is discussed in references 27-29.

Raju and Newman (ref. 28) used about 9000 degrees of freedom in their finite element model while Nishioka and Atluri (ref. 76) used about 1400 degrees of freedom in the finite-element-alternating method. The accuracy of the two solutions appears to be comparable. The efficiency of the new finite-element-alternating method appears to be attributable to the complete analytical solution of references 16 and 17.

CONCLUDING REMARKS

In the design of damage tolerant structures, complex three-dimensional (3-D) configurations with cracks are encountered. For a safe design, accurate stress-intensity factor solutions are needed. Until the early 70's, the complex 3-D configurations were approximated as two-dimensional (2-D) configurations. However, recent advances in the methods to solve the 3-D boundary-value problems and the development of large, fast computers have lead to more accurate modeling of these complex configurations. In this paper, various

methods that are available to solve 3-D boundary-value problems and the techniques used to obtain mode-I stress-intensity factors are reviewed.

The most widely used method is the finite-element method. Several types of singularity elements were proposed for 3-D crack problems. The most attractive of these appears to be the family of quarter-point elements. These elements can be easily implemented in general purpose programs. In general, the major difficulty with the finite-element methods is the effort involved in modeling the solid. But even this difficulty is being circumvented by the recent advances in automatic mesh generators. On the other hand, the boundary-integral equation (BIE) method needs only modeling of the surfaces of the solid and so is gaining popularity.

The line-spring model appears to be the fastest way to obtain good estimates of the stress-intensity factors. However, this model requires a specialized program. Recent literature shows that some versions of general purpose programs like ADINA have the line-spring elements in their library of finite elements.

The most accurate solution at the minimum cost appears to be provided by the finite-element-alternating method. The success of the method is due to the recent analytical solution of an embedded elliptical crack subjected to arbitrary pressure loading. Again, the major disadvantage is that this method needs a specialized computer program module for the analytical solution. Presently, such a module is not available to the general user. However, investment of time and effort in the development of the module is certainly worthwhile. A further disadvantage of this method is that it is applicable only to crack shapes which are elliptical or part elliptical.

After the stress analysis of a 3-D crack problem is completed, the stress-intensity factor needs to be extracted from the solution. Several

investigators have proposed singularity elements which yield stress-intensity factors as a part of the solution. These elements are the enriched elements, stress-hybrid and displacement-hybrid elements. However, with other finite-element methods and the BIE method, three methods are generally used to extract the stress-intensity factors. They are the crack-opening displacement (COD) method, the force method, and the virtual crack-extension method. Of the three, the COD method and the virtual crack extension method are widely used. In fact, comparisons between various stress-intensity factor solutions for several 3-D crack problems show that all three methods yield nearly identical solutions when plane-strain conditions exist at the crack fronts.

In general, despite the complexity of some crack configurations, comparisons between the available methods have shown that accurate mode-I stress-intensity factors can be obtained. The choice of a particular method is governed only by the availability of computer programs and resources to obtain the solution. As analyses of the 3-D crack configurations are completed, compendia of stress-intensity factors like the ones that are available for 2-D configurations, can be developed. With the advent of supercomputers, and with the reduction and anticipated reduction in computing costs, such compendia appear to be within the researchers' reach. Some investigators have already made efforts in this direction. The compendia can help engineers design structural components which are safe, economical and damage tolerant.

APPENDIX

Mixed Methods

The following three mixed methods are presented in this appendix.

1. Superposition of analytical and finite element methods.
2. Stress-difference method.
3. Discretization error method.

Superposition of Analytical and Finite Element Methods

Yamamoto and Sumi (refs. 98, 99) proposed the use of the method of superposition of analytical and finite element solutions. The singular part of the solution around a crack front is expressed as a linear combination of analytical solutions. The stress-intensity factor is determined by a linear combination of finite element and analytical solutions. References 98 and 99 applied the technique to compact specimens, round bars with circumferential cracks, and surface cracks in plates.

Yagawa and Nishioka (ref. 92) divide the total solid into two regions: the inner region and the outer region. The inner region V_1, is the region which surrounds the crack front and the remainder of the solid is represented by the outer region V_0. The displacements in the two regions are

$$u^{(0)} = \hat{u}^{(0)} \quad \text{in} \quad V_0$$

and

$$u^{(1)} = \hat{u}^{(1)} + \tilde{u} \quad \text{in} \quad V_1 \tag{17}$$

where $\hat{u}^{(0)}$ and $\hat{u}^{(1)}$ are the usual finite element displacements and $\tilde{u}$ are the displacements due to the analytical solution (s).

The displacements $\tilde{u}$ are taken as the product of plane-strain solutions in planes normal to the crack plane (in r, θ coordinates) and a power series in s, the coordinate along the crack front.

$$\tilde{u} = f(s)\tilde{u}_p(r,\theta) = \left[\sum_m a_m s^m\right]\tilde{u}_p(r,\theta) \tag{18}$$

The generalized displacements a_m, $\hat{u}^{(0)}$, and $\hat{u}^{(1)}$, are the unknown displacements in the problem. These are determined by minimizing the total potential energy of the system.

Yamamoto and Nishioka (ref. 92) applied this method to the embedded penny-shaped crack and semi-circular surface crack problems. They showed good comparisons with known solutions.

Stress-Difference Method

In this method, successive finite-element solutions are used to obtain stress-intensity factors (ref. 100). Two finite-element solutions with identical mesh patterns are obtained, one with no crack (i.e., crack completely closed) and the other with the crack. Let the stress σ_g be the stress in an element at a hypothetical crack tip in the solid with no crack (crack completely closed). With the same finite element model, let σ_{tip} be the stress in the same element in the solid with the crack. The stress difference $(\sigma_{tip} - \sigma_g)$ at the crack-tip element is assumed to be related to the stress-intensity factor. Two problems A and B are solved with this procedure. Then, for the two problems A and B the stress-difference ratio $(\sigma_{tip} - \sigma_g)_A/(\sigma_{tip} - \sigma_g)_B$ will be nearly equal to the ratio of stress-intensity factors K_A/K_B at that location. Therefore, if one of the stress-intensity factors is known the other can be calculated. Reference 100 showed

good agreements for a limited number of 2-D and 3-D problems with known solutions.

Discretization Error Method

In this method, a combination of conventional finite-element solution and the discretization error of the mesh subdivision is used to determine stress-intensity factor (ref. 101). The finite element solution, f, can be represented as the sum of the exact solution, f_{ex}, and the discretization error, provided that the round-off error is negligible. Reference 101, assumes that

$$f = f_{ex} + \sum_{j=1}^{3} A_{x_j} N_{x_j}^{-\delta_{x_j}} \tag{19}$$

where A_j and N_j are the amplitude of the error and the number of elements, respectively. The δ_j are positive parameters relating to the discretization error due to $N_j (j = 1, 2, 3)$. As the singularity around a crack front is, in general, particular to the directions x_1 and x_2 (see fig. 18) δ_{x_3} may be much larger than δ_{x_1} and δ_{x_2}. Therefore, equation (19) reduces to

$$f = f_{ex} + A_{x_1} N_{x_1}^{-\delta_{x_1}} + A_{x_2} N_{x_2}^{-\delta_{x_2}} \tag{20}$$

Yagawa et al. (ref. 101) further assume that $\delta_{x_1} = \delta_{x_2} = \delta$ and that the ratio N_{x_1}/N_{x_2} is a constant. Equation (20) then reduces to

$$f = f_{ex} + A\, N^{-\delta} \tag{21}$$

Similarly, the stress-intensity factor can be expressed as

$$K = K_{ex} + A\, N^{-\delta} \tag{22}$$

The unknowns are K_{ex}, A, and δ. To determine K_{ex} from equation (22), three finite-element solutions are obtained with three different mesh sizes N_1, N_2, and N_3 resulting in three stress-intensity factors K_1, K_2, and K_3, respectively. The unknowns K_{ex}, A, and δ can then be determined by using the three equations,

$$K_i = K_{ex} + A N_i^{-\delta}, \quad i = 1, 2, 3 \tag{23}$$

The above procedure is repeated at various stations along the crack front to obtain the stress-intensity factor distribution. The stiffness derivative method (ref. 89) is used to evaluate the K values needed in equations (22) and (23).

The discretization error method requires only coarse models. Reference 101 applied the method to through crack and surface crack problems and showed good agreement with earlier solutions.

REFERENCES

[1] Rooke, D. P., Baratta, F. I., and Cartwright, D. J.: Simple methods of determining stress-intensity factors. Engineering Fracture Mechanics, Vol. 14, 1981, pp. 397-426.

[2] Cartwright, D. J.: Stress-intensity factor determination. In Developments in Fracture Mechanics - 1, G. G. Chell (ed), Applied Science, London, 1979, pp. 29-66.

[3] Hellen, T. K.: Numerical Methods in Fracture Mechanics. In Developments in Fracture Mechanics - 1, G. G. Chell (ed), Applied Science Publishers Ltd, London, 1979, pp. 145-181.

[4] Tada, H., Paris, P. C., and Irwin, G. R.: The Stress Analysis of Cracks Handbook, Del Research Corp., 1973.

[5] Rooke, D. P., and Cartwright, D. J.: Compendium of Stress-Intensity Factors, London, HMSO, 1976.

[6] Sih, G. C.: Handbook of Stress-Intensity Factors - Stress-Intensity Factors Solutions and Formulas for Reference, Vol. 1 and 2, Institute of Fracture and Solid Mechanics, Lehigh University, Bethlehem, PA, 1973.

[7] Gran, R. J., Orazio, F. D., Paris, P. C., Irwin, G. R., and Hertzberg, R. H.: Investigation and analysis development of early life aircraft structural failures. AFFL-TR-70-149, Air Force Flight Laboratory, 1971.

[8] Panasynk, V. V., Andrejkiv, A. E., and Standik, M. M.: Three-dimensional static crack problem solutions (a review). Engineering Fracture Mechanics, Vol. 14, 1981, pp. 245-260.

[9] Parameter, R. R.: Stress-intensity factors for three-dimensional problems. AFRPL-TR-76-30, Air Force Rocket Propulsion Laboratory, 1976.

[10] Sneddon, I. N.: The distribution of stress in the neighborhood of a crack in an elastic solid. Proc. Royal Society of London, Series A, Vol. 187, 1946, pp. 229-260.

[11] Smith, F. W., Kobayashi, A. S., and Emery, A. F.: Stress intensity factors for penny-shaped cracks, Part I - infinite solid. Trans. ASME, Series E, Jnl. of Applied Mechanics, Vol. 89, 1967, pp. 947-952.

[12] Green, A. E., and Sneddon, I. N.: The distribution of stress in the neighborhood of a flat elliptical crack in an elastic solid. Proc. Cambridge Philosophical Society, Vol. 46, 1950, pp. 159-164.

[13] Irwin, G. R.: Crack-extension force for a part-through crack in a plate. Trans. ASME, Series E, Jnl. of Applied Mechanics, Vol. 84, 1962, pp. 651-654.

[14] Kassir, M. K., and Sih, G. C.: Three-dimensional stress distribution around an elliptical crack under arbitrary loadings. Trans. ASME, Series E, Jnl. of Applied Mechanics, Vol. 88, 1966, pp. 601-611.

[15] Shah, R. C., and Kobayashi, A. S.: Stress-intensity factors for an elliptical crack under arbitrary loading. Engineering Fracture Mechanics, Vol. 3, 1971, pp. 71-96.

[16] Vijayakumar, K., and Atluri, S. N.: An embedded elliptical flaw in an infinite solid subjected to arbitrary crack-face tractions. Trans. ASME, Series E, Jnl. of Applied Mechanics, Vol. 48, 1981, pp. 88-96.

[17] Nishioka, T., and Atluri, S. N.: Analytical solution for embedded elliptical cracks, and finite element alternating method for elliptical surface cracks, subjected to arbitrary loadings. Engineering Fracture Mechanics, Vol. 17, No. 3, 1983, pp. 247-268.

[18] Miyamoto, H., and Miyoski, T.: Analysis of stress-intensity factors for surface cracked tension plate, Proc. of Symposium on High Speed Computing of Elastic Structures, Liege, Belgium, 1971, Vol. 1, pp. 137-155.

[19] Chan, S. K., Tuba, I. S., and Wilson, W. K.: On the finite element in linear fracture mechanics. Engineering Fracture Mechanics, Vol. 2, 1970, pp. 1-17.

[20] Ando, Y., and Yagawa, G.: Recent developments in finite element method of three-dimensional crack problems in Japan. Proc. Int. conf. on Fracture Mechanics and Technology, Hong Kong, Sijthoff and Noordhoeff publishers, Vol. 2, 1977, pp. 1513-1528.

[21] Hall, C. A., Raymund, M., and Palusamy, S.: A macro element approach to computing stress-intensity factors for three-dimensional structures. Int. Jnl. of Fracture, Vol. 15, 1979, pp. 231-245.

[22] McGowan, J. J.: (Ed), A critical evaluation of numerical solutions to the "Benchmark" surface crack problem, SESA Monograph, 1980.

[23] McGowan, J. J., and Raymund, M.: Stress-intensity factor solutions for internal longitudinal semi-elliptical surface flaws in a cylinder under arbitrary loadings. Fracture Mechanics, C. W. Smith (Ed), ASTM STP 677, American Society for Testing of Materials, 1979, pp. 365-380.

[24] Tracey, D. M.: Finite elements for three-dimensional elastic crack analysis. Nuclear Engineering and Design, Vol. 26, 1974, pp. 282-290.

[25] Tracey, D. M.: Three-dimensional elastic singularity elements for evaluation of stress-intensity factor along an arbitrary crack front. Int. Jnl. of Fracture, Vol. 9, 1973, pp. 340-343.

[26] Raju, I. S., and Newman, J. C., Jr.: Three-dimensional finite element analysis of finite-thickness fracture specimens. NASA TN D-8414, National Aeronautics and Space Administration, 1977.

[27] Raju, I. S., and Newman, J. C., Jr.: Improved stress-intensity factors for semi-elliptic surface cracks in finite thickness plates. NASA TM X-72825, National Aeronautics and Space Administration, Washington, DC, 1977.

[28] Raju, I. S., and Newman, J. C., Jr.: Stress-intensity factors for two-symmetric corners cracks. Fracture Mechanics, C. W. Smith (Ed), ASTM STP 677, American Society for Testing of Materials, 1979, pp. 411-430.

[29] Raju, I. S., and Newman, J. C., Jr.: Stress-intensity factors for a wide range of semi-elliptical surface cracks in finite thickness plates. Engineering Fracture Mechanics, Vol. 11, 1979, pp. 817-829.

[30] Newman, J. C., Jr., and Raju, I. S.: Analysis of surface cracks in finite plates under tension and bending loads. NASA TP 1578, National Aeronautics and Space Administration, 1979.

[31] Newman, J. C., Jr., and Raju, I. S.: Stress-intensity factors for internal surface cracks in cylindrical pressure vessels. Trans. ASME, Jnl. of Pressure Vessel Technology, Vol. 102, 1980, pp. 342-346.

[32] Raju, I. S., and Newman, J. C.: Stress-intensity factors for internal and external surface cracks in cylindrical vessels. Trans. ASME, Jnl. of Pressure Vessel Technology, Vol. 104, 1982, pp. 293-298.

[33] Stern, M., and Becker, E. B.: A conforming crack tip element with quadratic variation in the singular terms. Int. Jnl. of Numerical Methods in Engineering, Vol. 12, 1978, pp. 279-288.

[34] Blackburn, W. S., and Hellen, T. K.: Calculation of stress-intensity factors in three-dimensions by finite element method. Int. Jnl. of Numerical Methods in Engineering, Vol. 11, 1979, pp. 211-229.

[35] Benzley, S. E.: Representation of singularities in the isoparametric finite elements. Int. Jnl. Numerical Methods in Engineering, Vol. 8, 1974, pp. 537-545.

[36] Gifford, L. N., and Hilton, P. D.: Stress-intensity factors by enriched finite elements. Engineering Fracture Mechanics, Vol. 10, 1978, pp. 485-496.

[37] Hilton, P. D., Kiefer, B. V., and Sih, G. C.: Special finite element procedures for three-dimensional crack problems. Num. Meth. in Fracture Mechanics, Proc. of First Int. Conf., Swansea, Wales, 1978, A. R. Luxmoore and D. R. J. Owens (Eds), Pineridge Press, 1978, pp. 411-421.

[38] Hilton, P. D., and Kiefer, B. V.: The enriched element for finite element analysis of three-dimensional elastic crack problems. ASME Trans., Jnl. of Pressure Vessel Technology, Vol. 102, 1980, pp. 347-352.

[39] Hilton, P. D.: A specialized finite element approach for three-dimensional crack problems. In Plates and Shells with cracks, Leiden, Noordhoff Int. Publishing, 1977, pp. 273-298.

[40] Henshell, R. D., and Shaw, K. G.: Crack tip finite elements are unnecessary. Int. Jnl. Numerical Methods in Engineering, Vol. 9, 1975, pp. 496-507.

[41] Barsoum, R. S.: On the use of isoparametric finite elements in linear fracture mechanics. Int. Jnl. of Numerical Methods in Engineering, Vol. 10, 1976, pp. 25-37.

[42] Barsoum, R. S.: Quarter-point elements in fracture mechanics. Recent Advances in Engineering Sciences, Proc. of the 14th Annual Meeting, Bethlehem, PA, 1977, pp. 925-932.

[43] Manu, C.: Quarter-point elements for curved crack fronts. Computers and Structures, Vol. 17, 1983, pp. 227-231.

[44] Harrop, L. P.: The optimum size of quarter-point crack tip elements, Int. Jnl. Numerical Methods in Engineering, Vol. 18, 1982, pp. 1101-1103.

[45] Ingraffea, A. R., and Manu, C.: Stress-intensity factor computation in three-dimensions with quarter-point elements. Int. Jnl. of Numerical Methods in Engineering, Vol. 15, 1980, pp. 1427-1445.

[46] Lynn, P. P., and Ingraffea, A. R.: Transition elements to be used with quarter-point elements. Int. Jnl. Numerical Methods in Engineering, Vol. 12, 1978, pp. 1031-1036.

[47] Hechmer, J. L., and Bloom, J. M.: Determination of stress-intensity factors for the corner-cracked hole using isoparametric singularity elements. Int. Jnl. of Fracture, Vol. 13, 1977, pp. 732-735.

[48] Wu, X. R.: Stress-intensity factors for semi-elliptical surface cracks subjected to complex crack face loadings. Engineering Fracture Mechanics, Vol. 19, 1984, pp. 387-405.

[49] Pian, T. H. H., and Moriya, K.: Three-dimensional crack element by assumed stress hybrid model. Recent Advances in Engineering Sciences. Proc. of the 14th Annual Meeting, Bethlehem, PA, 1977, pp. 913-917.

[50] Pian, T. H. H., and Moriya, K.: Three-dimensional fracture analysis by assumed stress hybrid elements. Num. Meth. in Fracture Mechanics, Proc. of First Int. Conf., Swansea, Wales 1978, A. R. Luxmoore and D. R. J. Owens (Eds), Pineridge Press, 1978, pp. 363-373.

[51] Kuna, M.: Three-dimensional elastic analysis of compact tension specimen with straight and curved crack points. Int. Jnl. of Fracture, Vol. 19, 1982, pp. R62-R67.

[52] Tong, P., and Atluri, S. N.: On hybrid finite element technique for crack analysis. Proc. Int. Conf. on Fracture Mechanics and Technology, Hong Kong, Sijthoff and Noordhoff publishers, Vol. 2, 1977, pp. 1445-1466.

[53] Atluri, S. N., and Kathiresan, K.: Stress analysis of typical flaws in aerospace structural components using three-dimensional hybrid displacement finite element method. Proc. of 19th Structures and Structural Dynamics Conference, Bethesda, MD, April 3-5, 1978, pp. 340-350.

[54] Atluri, S. N., and Kathiresan, K.: An assumed displacement hybrid finite element model for three-dimensional linear elastic fracture mechanics analysis. Proc. of the 12th Soc. of Engineering Science Annual Meeting, Austin, TX, 1975, pp. 391-399.

[55] Atluri, S. N., Nakagaki, M., Kathiresan, K., Rhee, H. C., and Chen, W. H.: Hybrid finite element models for linear and nonlinear fracture mechanics. Num. Meth. in Fracture Mechanics, Proc. of First Int. Conf., Swansea, Wales, 1978, A. R. Luxmoore and D. R. J. Owens (Eds), Pineridge Press, 1978, pp. 52-66.

[56] Atluri, S. N., and Kathiresan, K.: Influence of flaw shape on stress-intensity factors for pressure vessel surface flaws and nozzle corners. Trans. ASME, Jnl. Pressure Vessel Technology, Vol. 102, 1980, pp. 278-286.

[57] Atluri, S. N., and Kathiresan, K.: 3-d analysis of surface flaws in thick walled reactor pressure vessels using displacement hybrid methods. Nuclear Engineering and Design, Vol. 51, 1979, pp. 163-176.

[58] Atluri, S. N., and Kathiresan, K.: Stress-intensity factors for arbitrary shaped flaws in reactor pressure vessel nozzle corners. Int. Jnl. Pressure Vessels and Piping, Vol. 8, 1980, pp. 313-332.

[59] Kathiresan, K.: Three-dimensional elastic fracture analysis by a displacement hybrid finite element model. Ph.D. Thesis, Georgia Institute of Technology, 1976.

[60] Rizzo, F. J.: An integral equation approach to boundary value problems of classical elastostatics. Quart. Jnl. of Applied Mathematics, Vol. 25, 1967, pp. 83-95.

[61] Cruse, T. A., and Rizzo, F. J.: A direct formulation and numerical solution of the general transient elastodynamic problem - I. Jnl. of Math. Analysis and Applications, Vol. 22, 1968, pp. 244-259.

[62] Cruse, T. A.: Application of boundary-integral equation method to three-dimensional stress analysis. Computers and Structures, Vol. 3, 1973, pp. 509-527.

[63] Brebbia, C. A.: The Boundary Element Method for Engineers, John-Wiley, Pentech Press, 1978.

[64] Banerjee, R. K., and Butterfield, R.: Developments in Boundary Element Methods, Applied Science Publishers, London, 1979.

[65] Cruse, T. A.: Numerical evaluation of elastic stress-intensity factors by the boundary-integral equation method. In The Surface Crack: Physical Problems and Computational Solutions, J. L. Swedlow (Ed), ASME, 1972, pp. 153-170.

[66] Heliot, J., Labbens, R., and Pellissier-Tanon, A.: Application of the boundary-integral equation method to three-dimensional crack problems. ASME Century 2 Pressure Vessel and Piping Conference, San Francisco, CA, Aug. 12-15, 1980.

[67] Heliot, J., Labbens, R. C., and Pellissier-Tanon, A.: Semi-elliptical surface cracks subjected to stress gradients. Fracture Mechanics, C. W. Smith (Ed), ASTM STP 677, American Society for Testing of Materials, 1979, pp. 341-364.

[68] Cruse, T. A., and Wilson, R. B.: The use of singularity functions in boundary-integral equation fracture mechanics modeling. Recent Advances in Engineering Sciences, Proc. of the 14th Annual Meeting, Bethlehem, PA, 1977, pp. 919-924.

[69] Harris, D. O., and Lin, E. Y.: Stress-intensity factors for complete circumferential interior surface cracks in hollow cylinders. Proc. of the 13th National Symposium on Fracture Mechanics, ASTM STP-743, pp. 375-386, 1980.

[70] Cruse, T. A., and Vanburen, W.: Three-dimensional elastic stress analysis of a fracture specimen with an edge crack. Int. Jnl. of Fracture Mechanics, Vol. 1, 1971, pp. 1-15.

[71] Lange, D.: 3-d fracture analysis using the boundary integral equation method. Num. Meth. in Fracture Mechanics, Proc. of the First Int. Conf., Swansea, Wales, 1978, A. R. Luxmoore and D. R. J. Owens (Eds), Pineridge Press, 1978, pp. 115-127.

[72] Shah, R. C., and Kobayashi, A. S.: On the surface flaw problem. In The Surface Crack: Physical Problems and Computational Solutions, J. L. Swedlow (Ed), ASME, 1972, pp. 79-124.

[73] Shah, R. C., and Kobayashi, A. S.: Elliptical crack in a finite-thickness plate subjected to tensile and bending loading. Trans. ASME, Jnl. of Pressure Vessel Technology, Vol. 96, 1974, pp. 47-54.

[74] Smith, F. W.: The elastic analysis of the part-circular surface flaw problem by the alternating method. In The Surface Crack: Physical Problems and Computational Solutions, J. L. Swedlow (Ed), ASME, 1972, pp. 125-152.

[75] Smith, F. W., and Alavi, M. J.: Stress-intensity factors for a penny-shaped crack in a half-space. Engineering Fracture Mechanics, Vol. 3, 1971, pp. 241-254.

[76] Nishioka, T., and Atluri, S. N.: An alternating method for analysis of surface-flawed aircraft structural components. AIAA Jnl., Vol. 21, 1983, pp. 749-757.

[77] Nishioka, T., and Atluri, S. N.: Analysis of surface flaw in pressure vessel by a new 3-dimensional alternating method. Trans. ASME, Jnl. of Pressure Vessel Technology, Vol. 104, 1982, pp. 299-307.

[78] Browning, W. M., and Smith, F. W.: An analysis technique for complex three-dimensional crack problems, Proc. of 8th Southeastern Conf. on Theoretical and Applied Mechanics, Blackburg, Virginia, 1976, pp. 141-150.

[79] Smith, F. W., and Kullgren, T. E.: Theoretical and experimental analysis of surface cracks emanating from fastener holes. AFFDL-TR-76-104, Air Force Flight Dynamics Laboratory, 1977.

[80] Rice, J. R., and Levy, N.: The part-through surface crack in an elastic plate. Trans. ASME, Series E, Jnl. of Applied Mechanics, Vol. 94, 1972, pp. 185-194.

[81] German, M. D., Kumar, V., and deLorenzi, H. G.: Analysis of surface cracks in plates and shells using the line-spring model and ADINA. Computers and Structures, Vol. 17, 1983, pp. 881-890.

[82] Parks, D. M., Lockett, R., and Brockenbrough, J. R.: Stress-intensity factors for surface-cracked plates and cylindrical shells using line-spring finite-elements. Proc. of the Winter Annual Meeting, ASME, Washington, DC, 1981, pp. 279-285.

[83] Delale, F., and Erdogan, F.: Application of line-spring model to a cylindrical shell containing a circumferential or axial part-through crack. Trans. ASME, Series E, Jnl. of Applied Mechanics, Vol. 49, 1982, pp. 97-102.

[84] Delale, F., and Erdogan, F.: Line-spring model for surface crack in a Reissner plate. Int. Jnl. of Engineering Science, Vol. 19, 1981, pp. 1331-1340.

[85] Rice, J. R.: The line spring model for the surface flaws. In The Surface Crack: Physical Problems and Computational Solutions, J. L. Swedlow (Ed), ASME, 1972, pp. 171-186.

[86] Dill, H. D., and Saff, C. R.: Environment-load interaction effects on crack growth. AFFDL-TR-78-137, Air Force Flight Dynamics Laboratory, 1978.

[87] Tseng, A. A.: A comparison of three-dimensional finite-element solutions for the compact specimen, Int. Jnl. of Fracture, Vol. 17, 1981, pp. R125-R129.

[88] Bloom, J. M., and van Fossen, D. B.: An evaluation of the 20-node quadratic isoparametric singularity brick elements. Int. Jnl. of Fracture, Vol. 12, 1976, pp. 161-163.

[89] Parks, D. M.: A stiffness derivative finite element technique for determination of crack tip stress-intensity factors. Int. Jnl. of Fracture, Vol. 10, 1974, pp. 487-502.

[90] Hellen, T. K.: On the method of virtual crack extensions. Int. Jnl. of Numerical Methods in Engineering, 1975, Vol. 9, pp. 187-207.

[91] Raju, I. S., and Newman, J. C., Jr.: Three-dimensional finite-element analysis of the chevron-notched fracture specimens. Paper presented at the ASTM Symposium on Chevron-Notched Specimens: Testing and Stress Analysis, April 21, 1983, Louisville, KY. (Available as NASA TM 85798, 1984.)

[92] Yagawa, G., and Nishioka, T.: Superposition method for semi-circular surface crack. Int. Jnl. of Solids and Structures, Vol. 16, 1980, pp. 585-595.

[93] Newman, J. C., Jr.: A review and assessment of the stress-intensity factors for surface cracks. In Part-Through Crack Fatigue Life Predictions, ASTM STP-687, J. B. Chang (Ed), American Society for Testing and Materials, 1979, pp. 16-42.

[94] Smith, F. W., and Sorensen, D. R.: Mixed mode stress-intensity factors for semi-elliptic surface crack. NASA CR-134684, National Aeronautics and Space Administration, 1974.

[95] Hulbert, L. E.: Benchmark problems for three-dimensional fracture analysis. Int. Jnl. of Fracture, Vol. 13, 1977, pp. 87-91.

[96] Heliot, J., Labbens, R., and Pellissier-Tanon, A.: Benchmark problem No. 1 - semi-elliptical surface crack results. Int. Jnl. of Fracture, Vol. 15, 1979, pp. R197-R202.

[97] Shah, R. C.: Stress-intensity factors for through and part-through cracks originating from fastener holes. In Mechanics of Crack Growth, ASTM STP 590, American Society for Testing and Materials, 1976, pp. 429-459.

[98] Yamamoto, Y., and Sumi, Y.: Stress-intensity factors for three-dimensional cracks. Int. Jnl. of Fracture, Vol. 14, 1978, pp. 17-38.

[99] Yamamoto, Y., and Sumi, Y.: Stress-intensity factors for three-dimensional cracks. Int. Union of Theoretical and Applied Mechanics, 14th Int. Conf. of Theoretical and Applied Mechanics, Delft, The Netherlands, Aug. 30 - Sept. 4, 1976.

[100] Mukurami, T.: A simple procedure for the accurate determination of stress-intensity factors by the finite element method. Num. Meth. in Fracture Mechanics, Proc. of the First Int. Conf., Swansea, Wales, 1978, A. R. Luxmoore and D. R. J. Owens (Eds), Pineridge Press, 1978, pp. 322-335.

[101] Yagawa, G., Ando, Y., and Ichimiya, M.: Two- and three-dimensional analyses of stress-intensity factors based on discretization errors in finite elements. Num. Meth. in Fracture Mechanics, Proc. of First Int. Conf., Swansea, Wales, A. R. Luxmoore and D. R. J. Owens (Eds), Pineridge Press, 1978, pp. 249-267.

Table 1.- Comparison of Stress-Intensity Factor Solutions by Various Investigators for Compact Specimens

$$F = \frac{K_I B\sqrt{W}}{P}; \quad \beta = \frac{F}{F_{collocation}}; \quad \nu = 0.3$$

Investigator(s)	C/W	Element Type	K-evaluation method	Degrees of Freedom	β	
					2-D plane strain	3-D at midplane
Tracey [25][a]	0.5	6-noded singular	COD Approach 1	1980	0.94	0.99
Raju & Newman [26][a]	0.5	6-noded singular	Force Method	1875	-	0.99
Tseng & Berry [87][a]	0.5	15-noded singular	COD Approach 1 COD Approach 2	1497 1497	0.99 0.95	1.08 1.05
Bloom & van Fossen [88][a]	0.5	20-noded Quarter-point	COD Approach 2	1200 4965	0.97 0.99	1.035 1.076
Tseng & Berry [87][a]	0.5	20-noded Quarter-point	COD Approach 1 COD Approach 2	1497 1497	0.97 0.94	1.07 1.04
de Lorenzi [87][b]	0.6	20-noded Quarter-point	COD Approach 2	4887	-	1.07
Kathiresan [59][b]	0.6	20-noded displ. hybrid	K-built in	1476	-	1.01
Pian & Moriya [50][b]	0.5	20-noded Stress hybrid	K-built in	504	-	1.08
Yamamoto & Sumi [98, 99][b]	0.5	20-node Isoparametric	Superposition	2106	0.99	1.08
Yagawa & Nishioka [92][b]	0.5	20-node Isoparametric	Superposition	376	1.00	1.07
Raju & Newman [91][c]	0.55	6-noded singular	Force Method	5085	0.98	1.08

[a]Configuration is Type A with W/B = 2.
[b]Configuration is Type B with W/B = 2.
[c]Configuration is Type C with W/B = 1 (see Fig. 10).

Table 2.- Convergence of the Finite Element Solution With Mesh Refinement in the Thickness Direction for a Compact Specimen - Type C (see Fig. 10)

$W/B = 2.0$; $F = \frac{K_I B\sqrt{W}}{P}$; $F_{\text{plane strain}} = 20.216$;

$a/W = 0.55$

Number of nodes on each Z = constant plane = 339

No. of Layers	Degrees of Freedom	$F_{\text{at midplane}}$	$\frac{F_{\text{midplane}}}{F_{\text{plane strain}}}$
2	3051	22.374	1.107
4	5085	22.566	1.116
8	9153	22.631	1.119

Table 3.- Effect of Thickness on the Stress-Intensity Factor at Midplane of a Compact Specimen (Type C) (see Fig. 10)

$$F = \frac{K_I B\sqrt{W}}{P}; \quad a/W = 0.55; \quad F_{\text{plane strain}} = 20.216$$

W/B	$F_{\text{at midplane}}$[a]	$F_{\text{midplane}}/F_{\text{plane strain}}$
5.0	21.818	1.079
2.0	22.566	1.116
1.0	21.854	1.081

[a]With 4-layer model in the thickness direction

Table 4.- Comparison of Stress-Intensity Factor Deepest Point ($\phi = \pi/2$) of a Semi-Elliptical Surface Crack in a Plate Subjected to Tension

$$a/c = 0.2; \quad F = K_I \Big/ \left\{ S\sqrt{\frac{\pi a}{Q}} \right\}$$

a/t	Finite Element Method Raju & Newman [28]	F at $\phi = \pi/2$		
		Line-Spring Models		
		German et al. [81][a]	Delale & Erdogan [84][b]	Dill & Saff [86][c]
0.2	1.173	1.173	-	1.174
0.4	1.359	1.404	1.365	1.425
0.6	1.642	1.692	1.635	1.655
0.8	1.851	1.865	1.841	1.820

[a]Values read from Fig. 6 of ref. 81.
[b]Values read from Fig. 7 of ref. 84.
[c]Values read from Fig. A-3 of ref. 86.

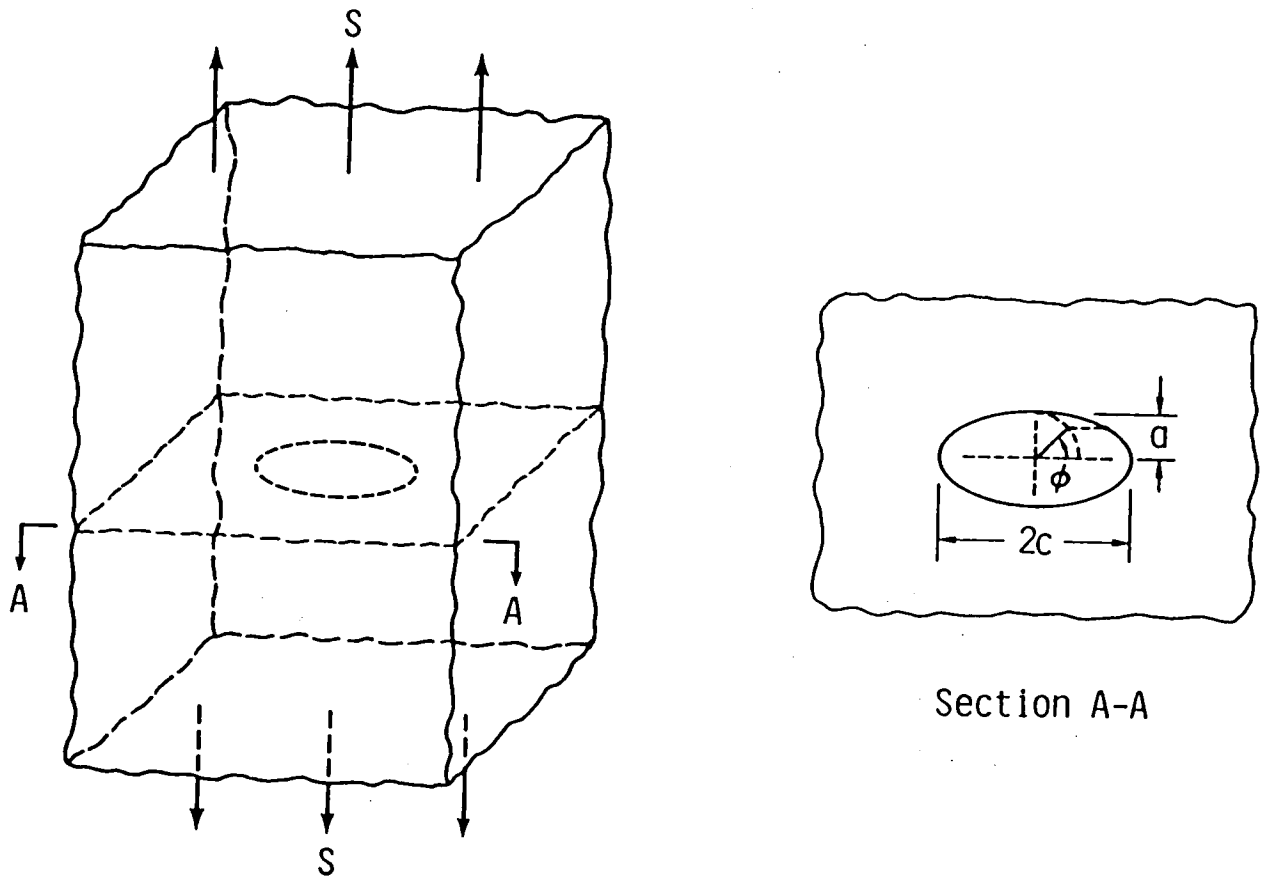

Fig. 1- Embedded elliptical crack in an infinite solid subjected to remote tension.

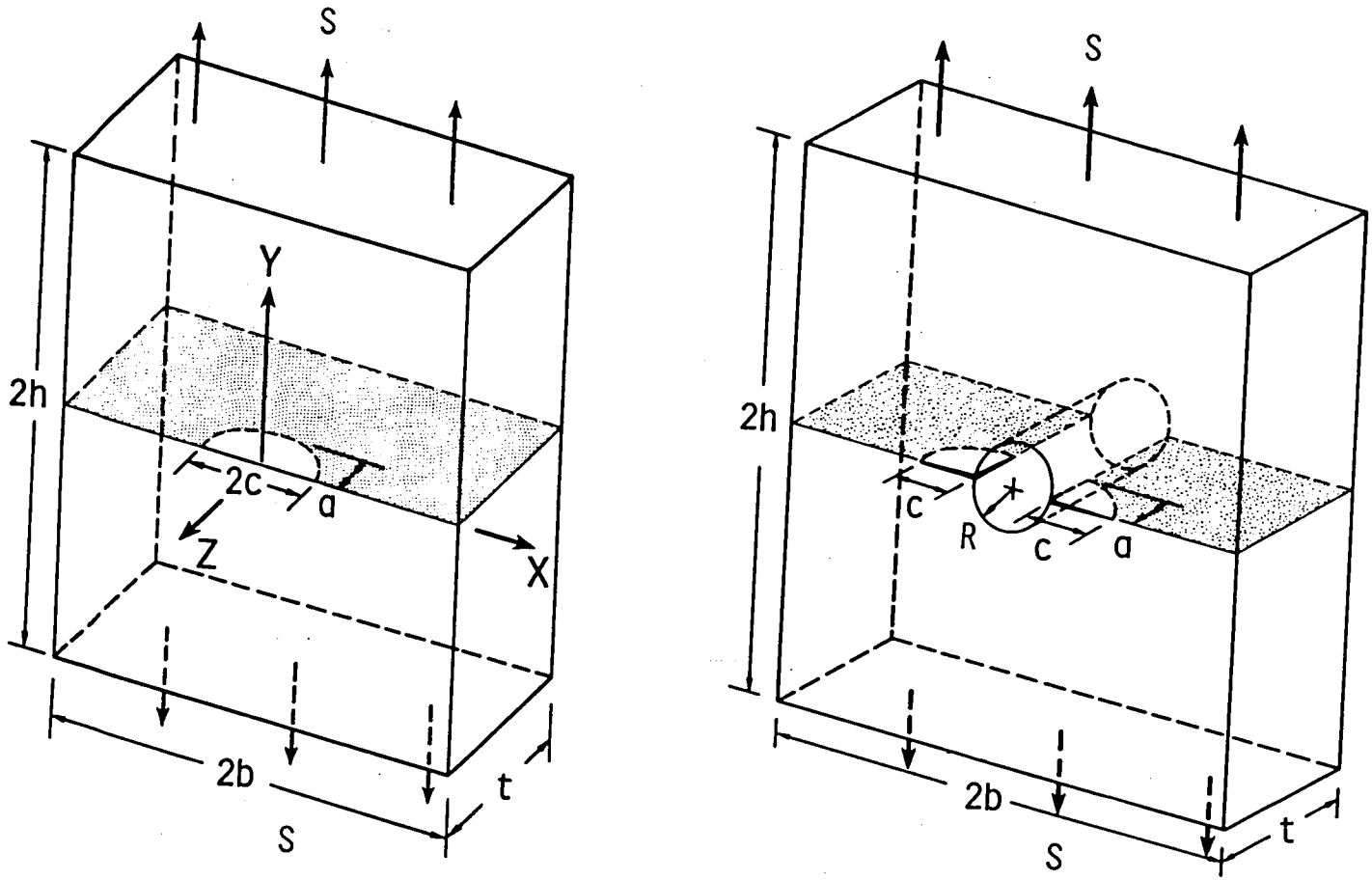

(a) Surface crack.

(b) Corner cracks at hole.

Fig. 2- Surface crack and corner crack from hole configurations.

Two-Dimensional Versions

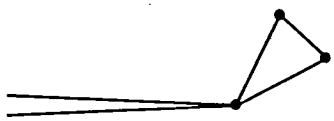

(a) 3-noded element, Tracey [24]

Three-Dimensional Versions

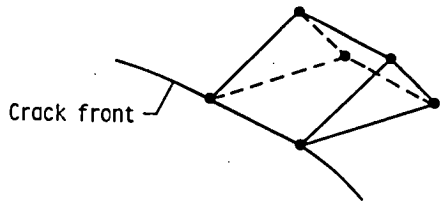

(b) 6-noded element, Tracey [24]

(c) 6-noded element,
Stern and Becker [33]

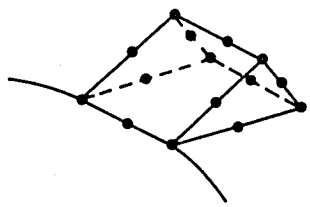

(d) 15-noded element,
Stern and Becker [33]
Blackburn and Hellen [34]
Hilton et al [37]

(e) 8-noded quarter-point element,
Henshell and Shaw [40]

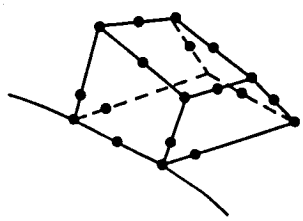

(f) 20-noded quarter-point element,
Henshell and Shaw [40]

(g) 6-noded quarter-point element,
Barsoum [41]

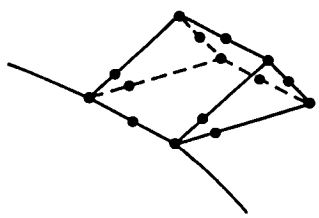

(h) 15-noded quarter-point element,
Barsoum [41]

Fig. 3- Various types of singularity elements.

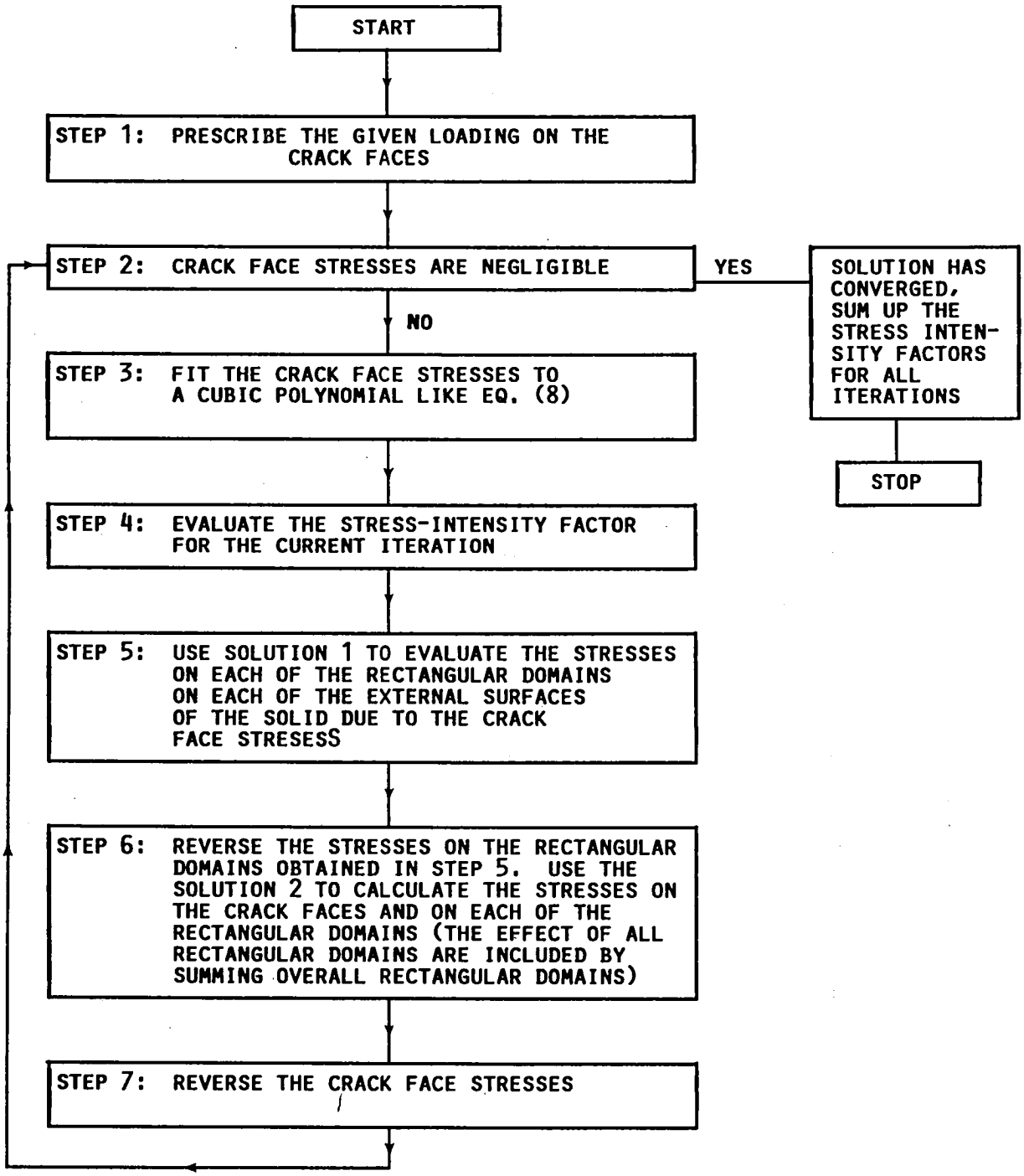

Fig. 4- Flow chart for the alternating method.

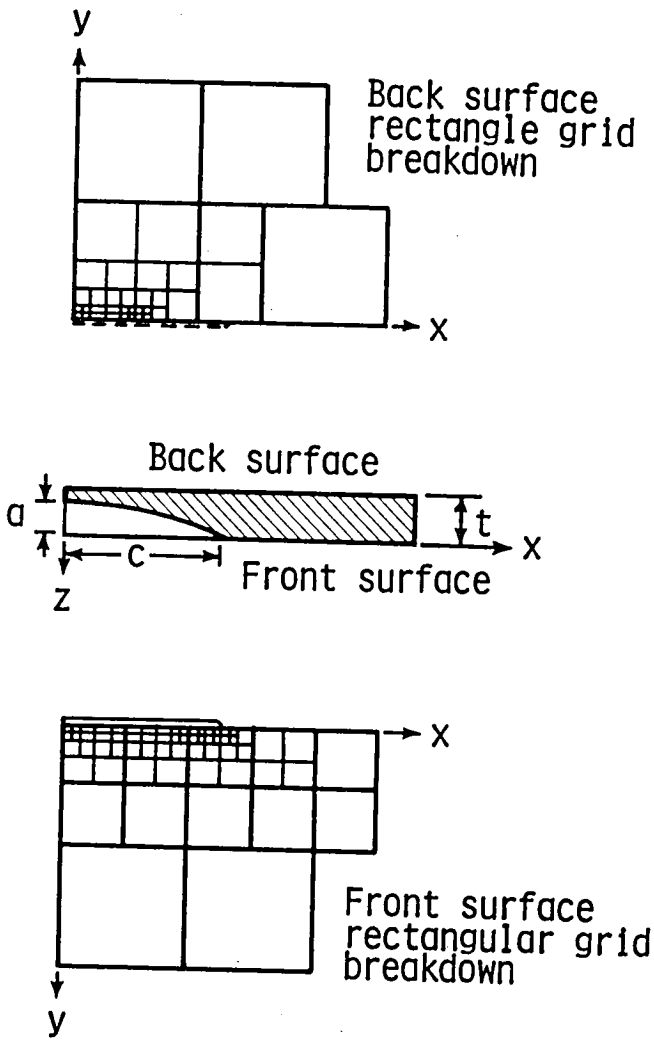

Fig. 5- Rectangular grid idealization for the front and back surfaces in the alternating method, ref. 72.

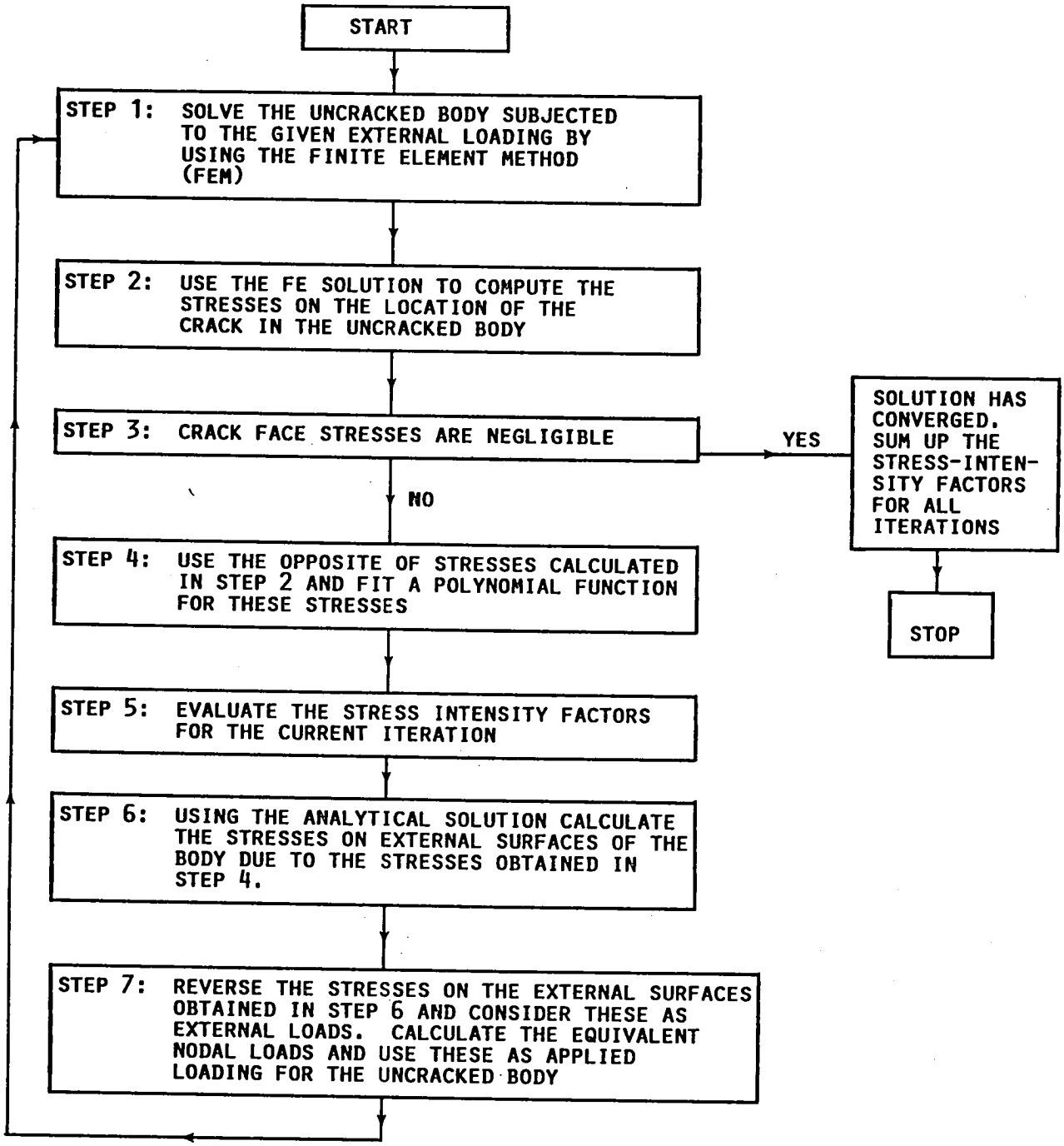

Fig. 6- Flow chart for the finite-element-alternating method.

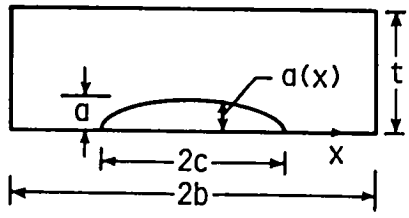

(a) Surface crack.

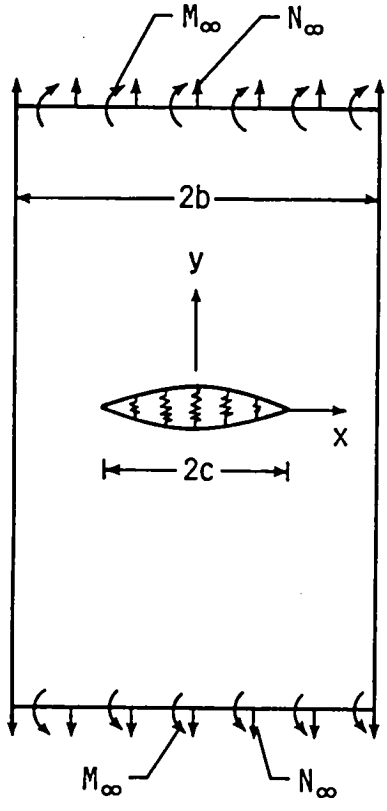

(b) Center crack with line springs across the crack faces.

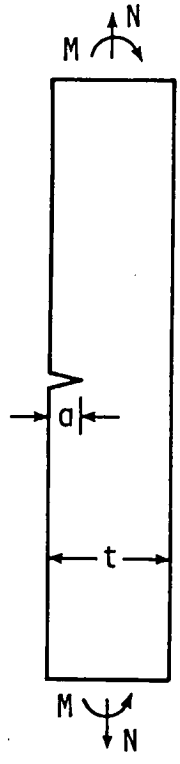

(c) Single-edge crack plate under plane strain.

Fig. 7- The line-spring model for the surface crack.

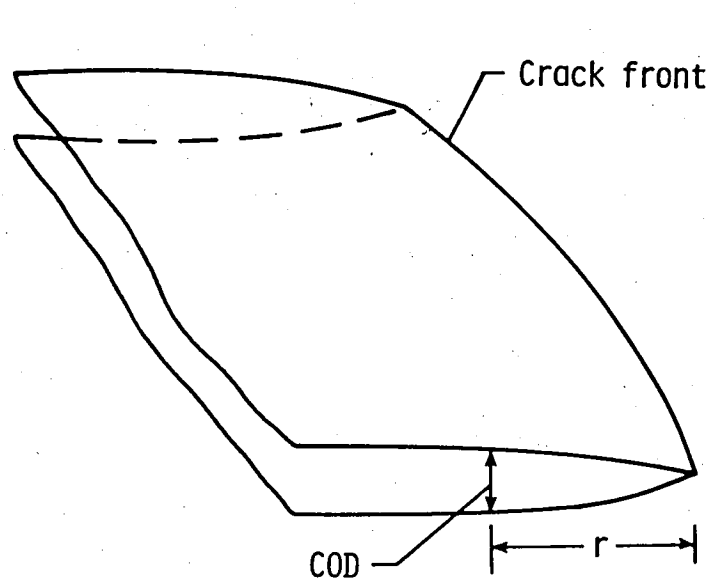

(a) Crack front region.

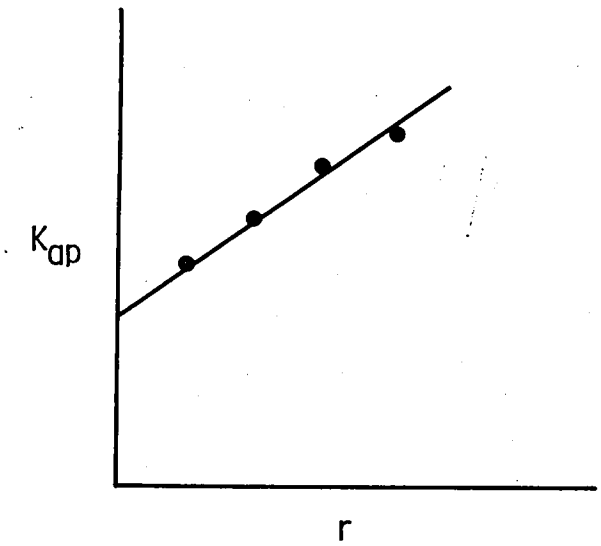

(b) Apparent stress-intensity factors.

Fig. 8- Crack-opening displacement method of evaluating stress-intensity factors.

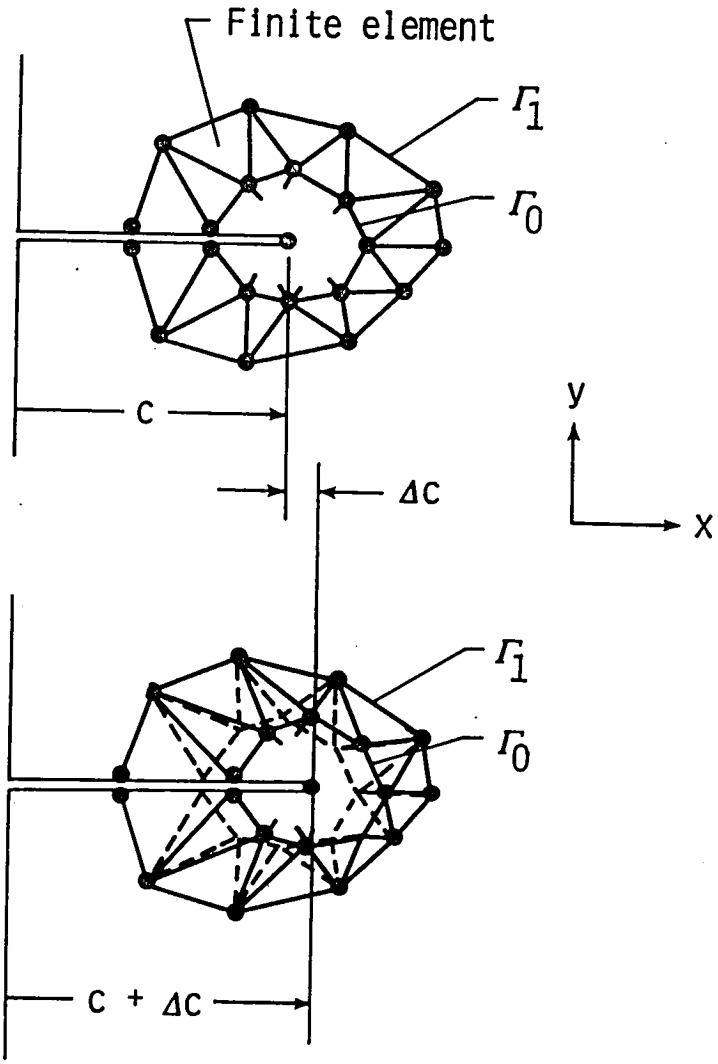

Fig. 9- Illustration of the virtual crack extension method.

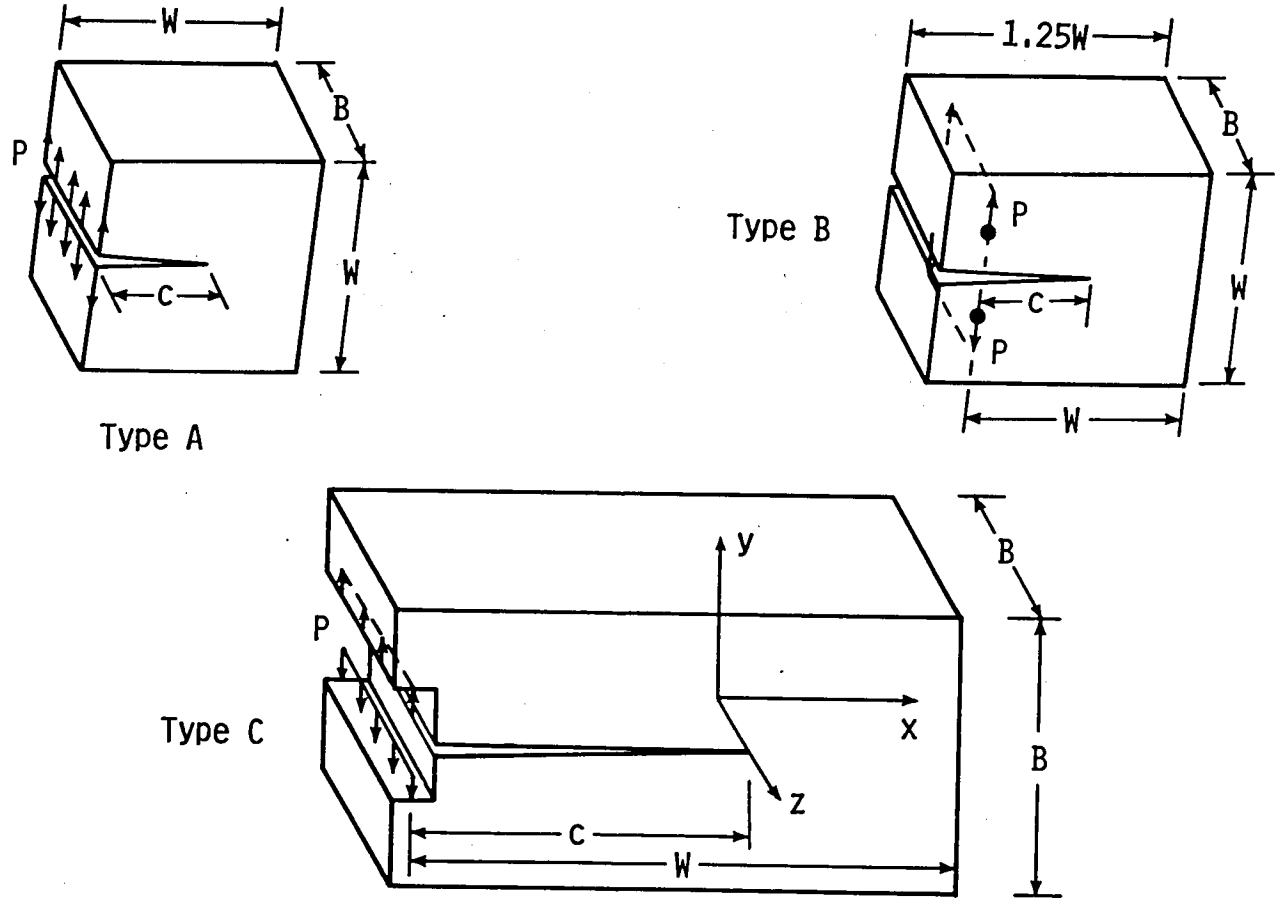

Fig. 10- Various compact type specimens analyzed.

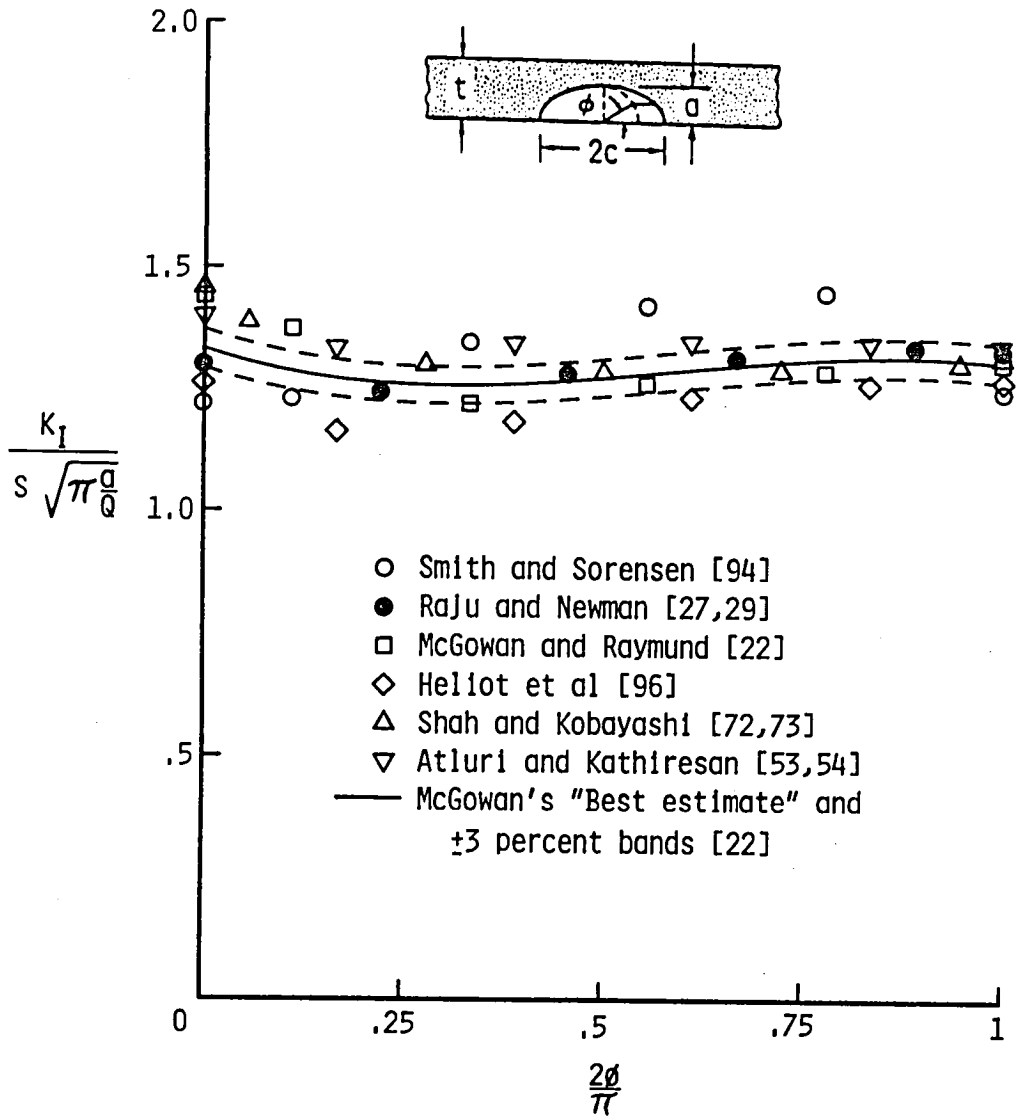

Fig. 11- Comparison of stress-intensity factors for a semi-elliptical surface crack in a plate subjected to remote tension (a/c = 0.5; a/t = 0.75).

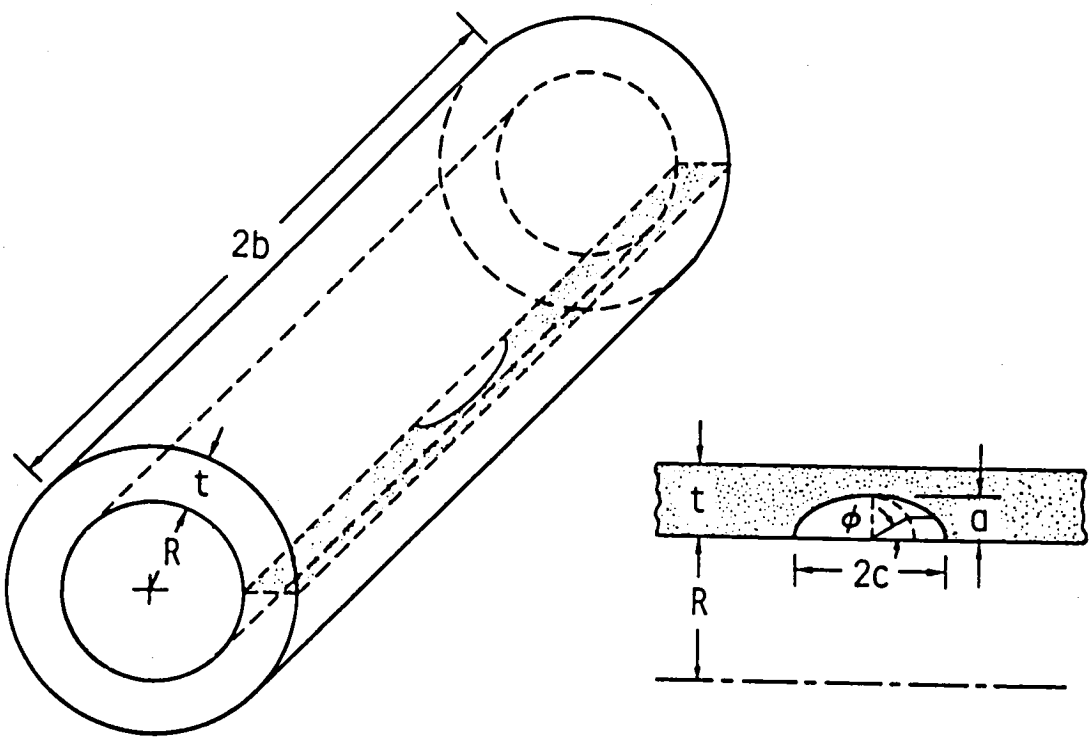

Fig. 12- Internal surface crack in a cylinder.

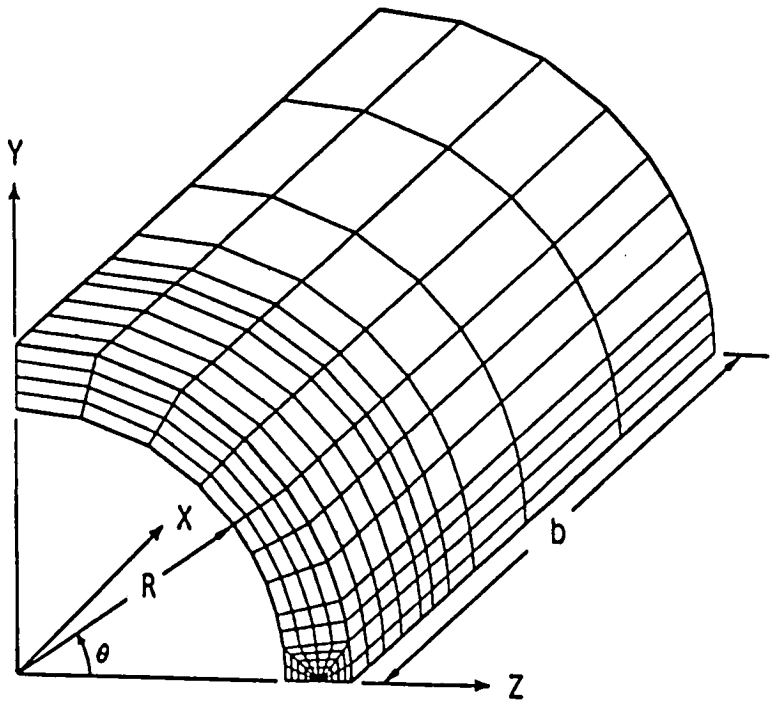

(a) Finite-element model.

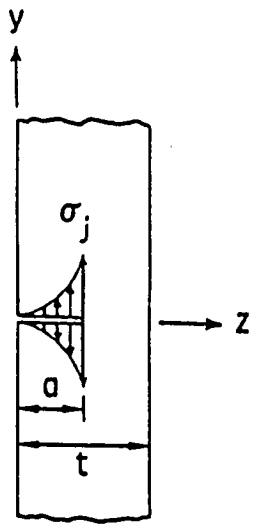

(c) Loading on crack surfaces.

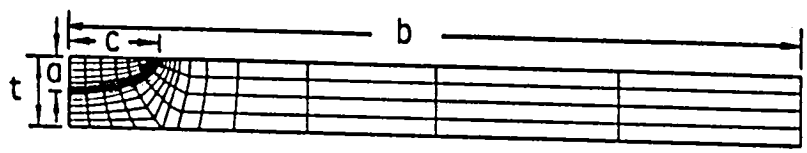

(b) Element pattern on Y = 0 plane.

Fig. 13- Finite-element model and loading on a semi-elliptical surface crack in a cylinder.

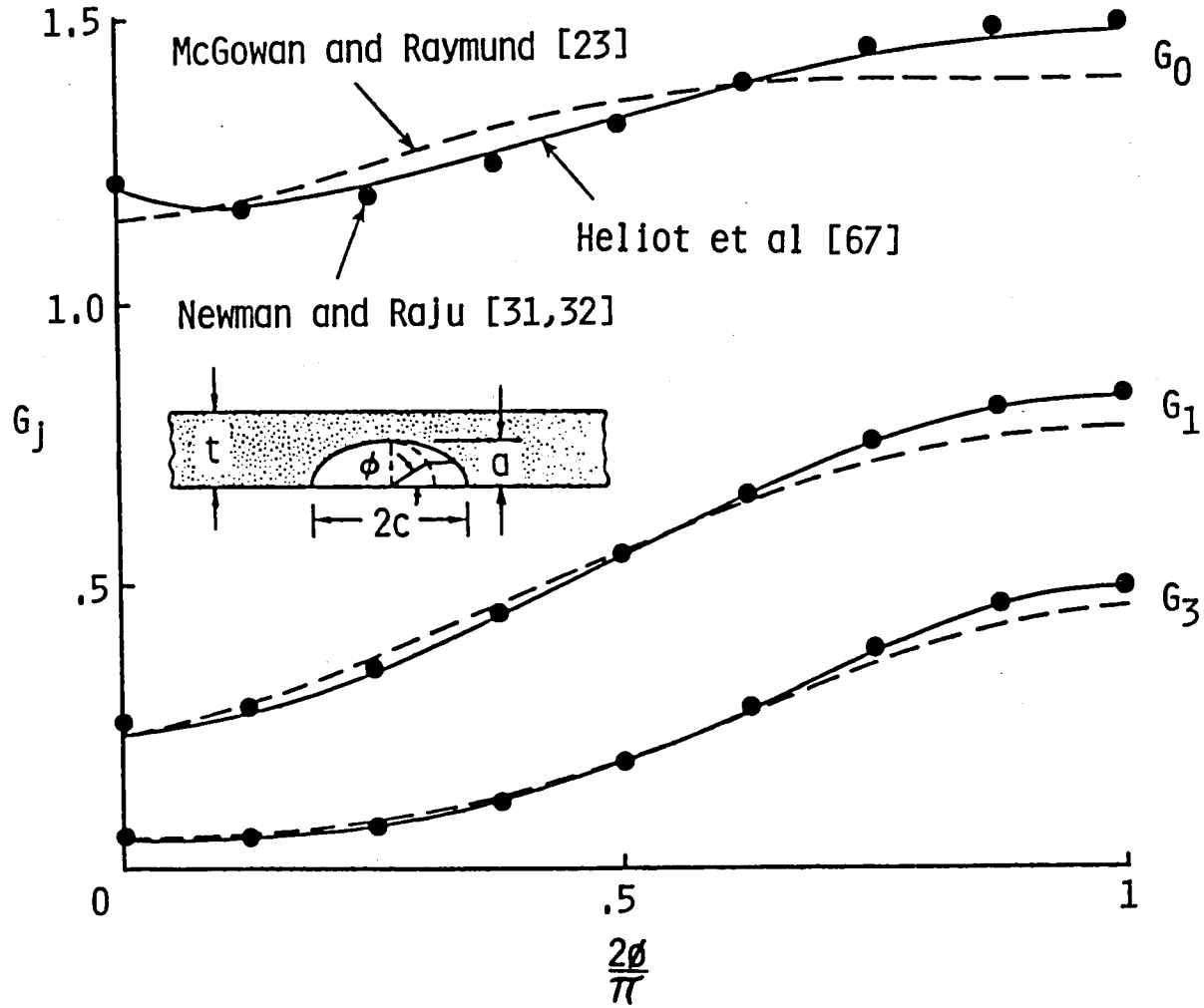

Fig. 14- Comparison of influence coefficients for an internal surface crack in a cylindrical vessel subjected to various crack surface load distributions (R/t = 10; a/c = 1/3; a/t = 0.8).

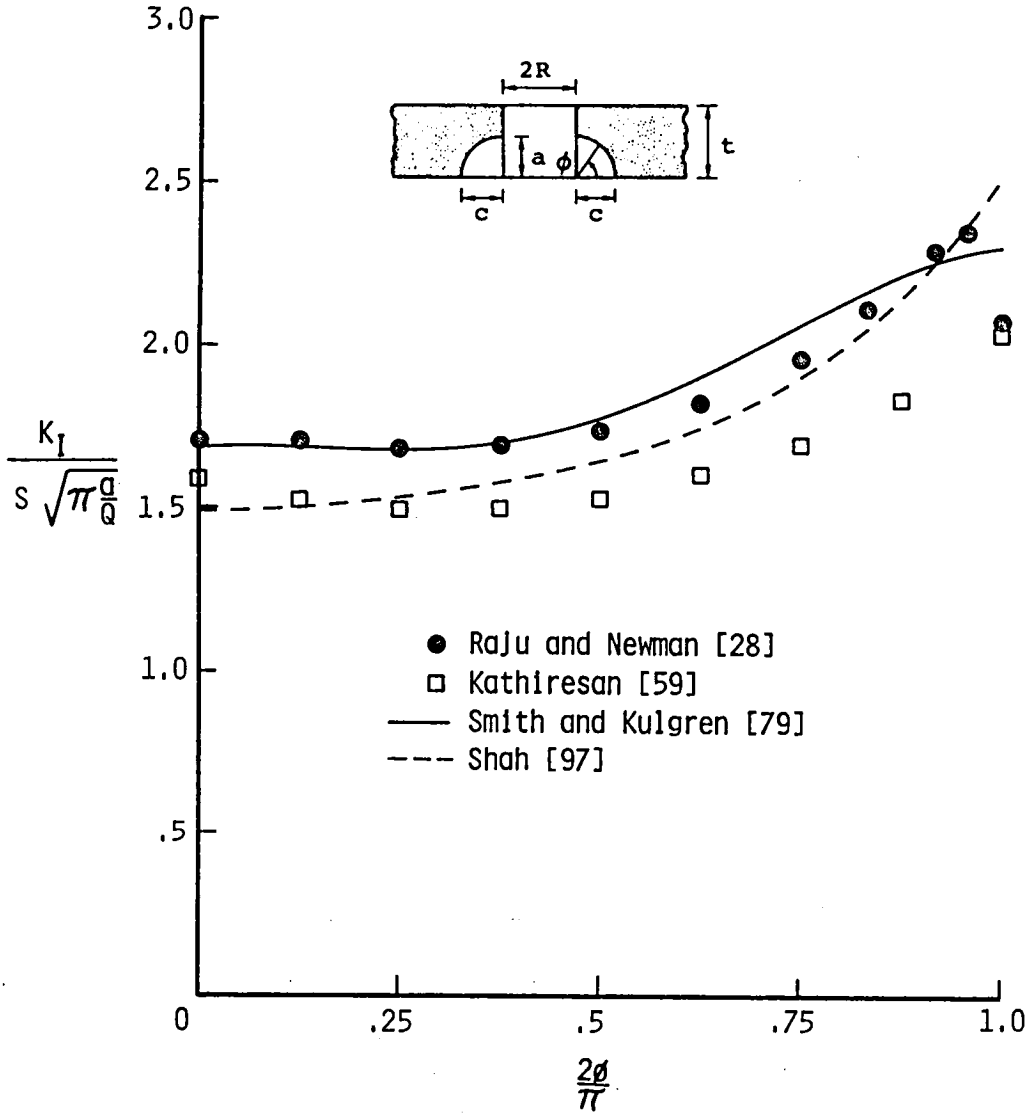

Fig. 15- Comparison of stress-intensity factors for corner cracks from a hole in a plate subjected to remote tension (R/t = 0.5; a/c = 1; a/t = 0.5).

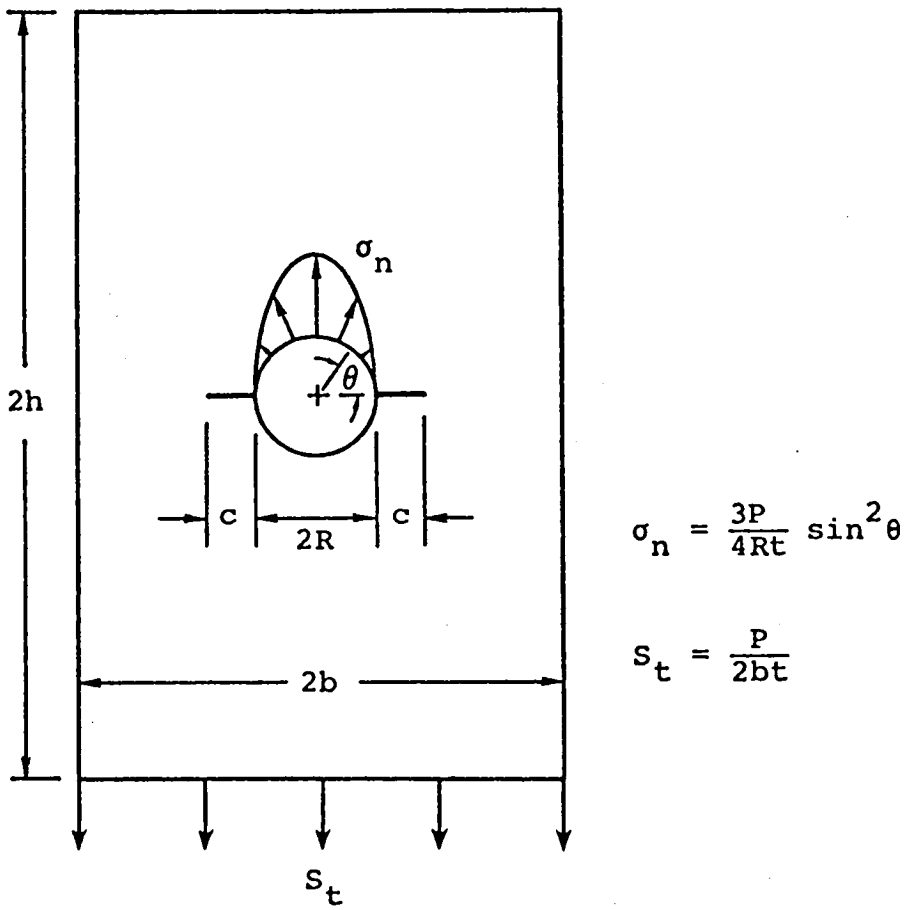

Fig. 16- Corner cracks from a hole in a plate subjected to pin loading.

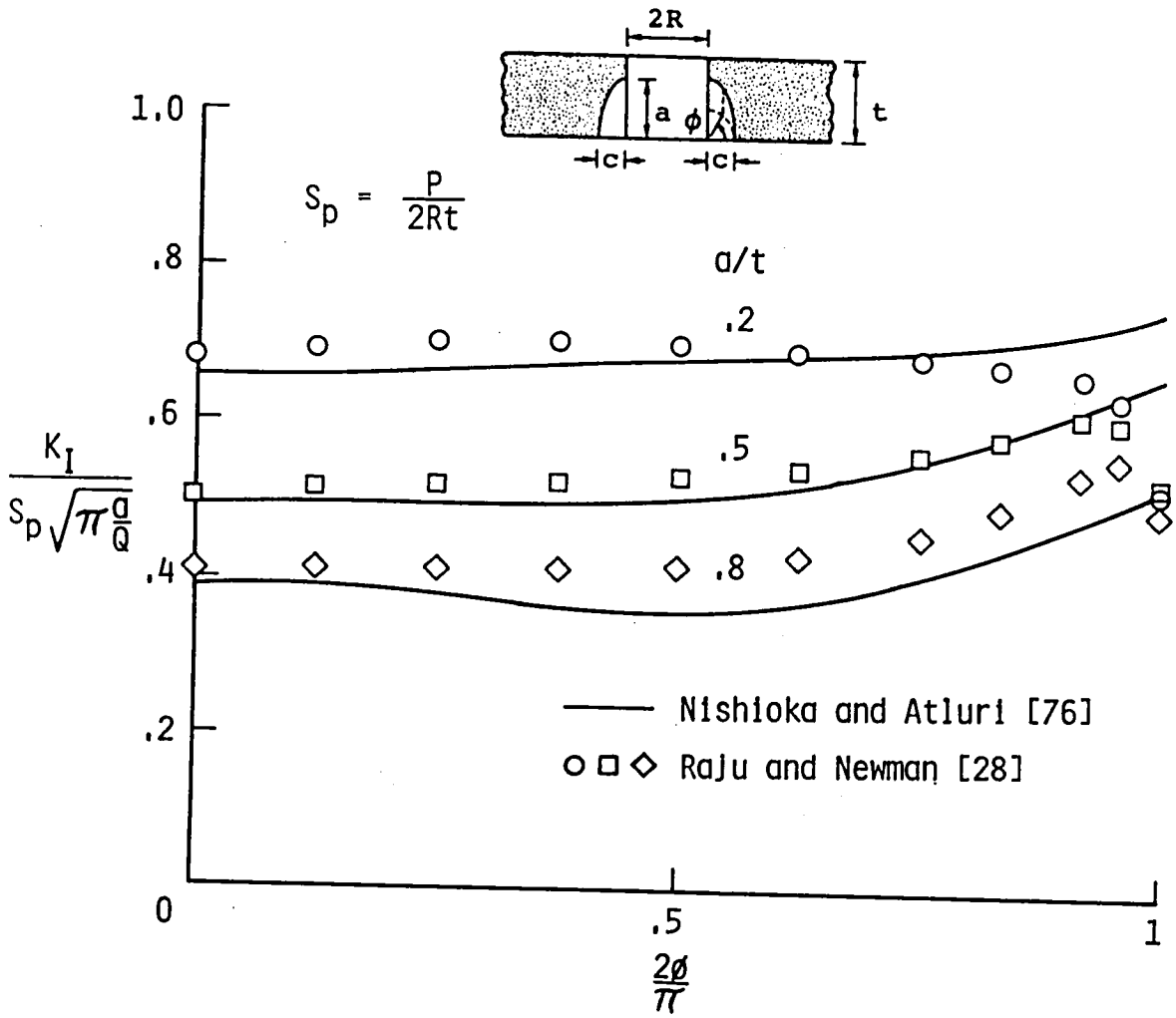

Fig. 17- Comparison of stress-intensity factors for corner cracks from a hole in a plate subjected to pin loading (R/t = 0.5; a/c = 2.0).

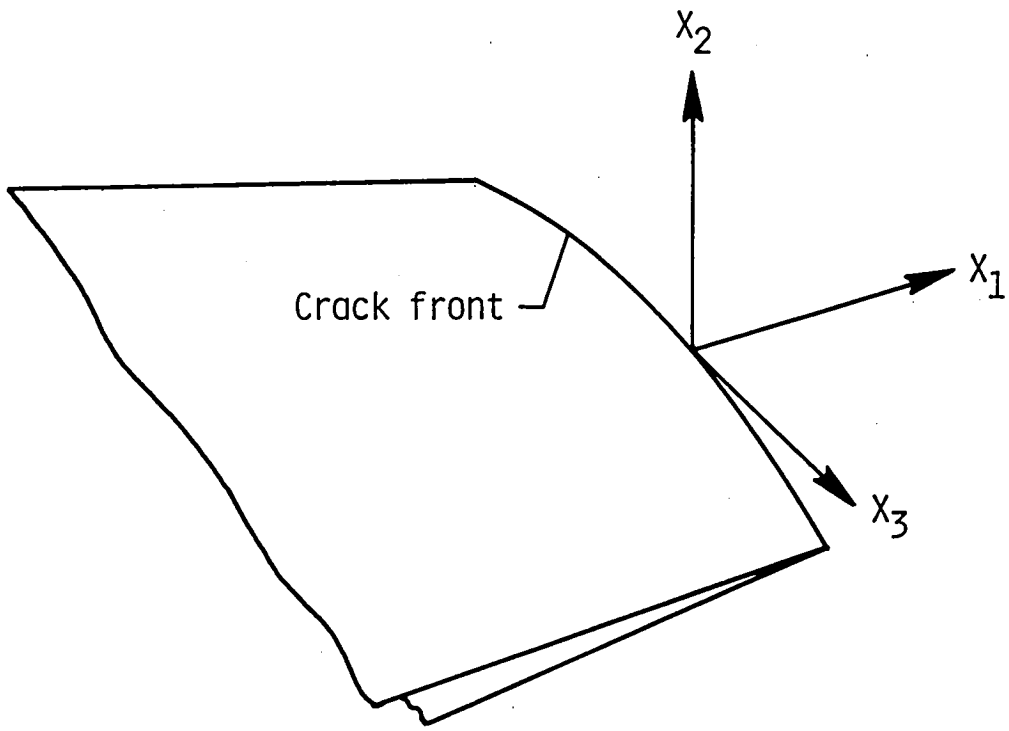

Fig. 18- Coordinate system used for the discretization-error method.

1. Report No.	2. Government Accession No.	3. Recipient's Catalog No.
NASA TM-86266		

4. Title and Subtitle	5. Report Date
METHODS FOR ANALYSIS OF CRACKS IN THREE-DIMENSIONAL SOLIDS	July 1984
	6. Performing Organization Code 505-33-23-02
7. Author(s)	8. Performing Organization Report No.
I. S. Raju and J. C. Newman, Jr.	
9. Performing Organization Name and Address	10. Work Unit No.
NASA Langley Research Center Hampton, VA 23665	11. Contract or Grant No.
12. Sponsoring Agency Name and Address	13. Type of Report and Period Covered
National Aeronautics and Space Administration Washington, DC 20546	Technical Memorandum
	14. Sponsoring Agency Code
15. Supplementary Notes	

16. Abstract

Various analytical and numerical methods used to evaluate the stress-intensity factors for cracks in three-dimensional (3-D) solids are reviewed. The review covers some of the classical exact solutions and many of the approximate methods used in 3-D analyses of cracks. The exact solutions for embedded elliptic cracks in infinite solids are discussed. The approximate methods reviewed are the finite element methods, the boundary-integral equation (BIE) method, the mixed methods (superposition of analytical and finite element method, stress-difference method, discretization-error method, alternating method, finite element-alternating method), and the line-spring model. The stress-intensity factor solutions for some commonly encountered 3-D crack configurations were compared. The solutions by various methods appear to show good agreement.

The finite-element method with singularity elements in the most widely used method. The BIE method only needs modeling of the surfaces of the solid and so is gaining popularity. The line-spring model appears to be the quickest way to obtain good estimates of the stress-intensity factors. The finite-element-alternating method appears to yield the most accurate solution at the minimum cost.

Comparisons between various methods have shown that accurate mode-I stress-intensity factors can be obtained. The choice of a particular method is only governed by the availability of computer programs and resources to obtain a solution.

17. Key Words (Suggested by Author(s))	18. Distribution Statement
Cracks Surface Cracks Corner Cracks Stress Analysis Finite-element method Boundary-integral method Elasticity Stress-intensity factors	Unclassified - Unlimited Subject Category 39

19. Security Classif. (of this report)	20. Security Classif. (of this page)	21. No. of Pages	22. Price
Unclassified	Unclassified	68	A04

N-305

For sale by the National Technical Information Service, Springfield, Virginia 22161